COMMUN. MATH. SCI.
Vol. 16, No. 6, pp. 1659–1684

INTERACTION OF THE ELEMENTARY WAVES OF ISENTROPIC FLOW IN A VARIABLE CROSS-SECTION DUCT*

WANCHENG SHENG† AND QINGLONG ZHANG‡

Abstract. The equations of fluid in a variable cross-section duct are nonconservative because of the source term. Recently, the Riemann solutions of the equations for the compressible duct flow have been obtained. The authors also obtained the elementary waves including rarefaction waves, shock waves and stationary wave. In this paper, we mainly discuss the interactions of rarefaction wave and shock wave with the stationary wave, for the cases in which the cross-section area is either decreasing or increasing. The large-time behavior is shown in each case.

Keywords. duct flow; nonconservative; interaction of elementary waves; Riemann problem.

AMS subject classifications. 35L65; 35L80; 35R35; 35L60; 35L50.

1. Introduction

When the cross-section area $a(x)$ does not change rapidly, a duct flow of an isothermal fluid in a nozzle can be seen as one dimensional flow. The equations are described as

$$\begin{cases} (a\rho)_t + (a\rho u)_x = 0, \\ (a\rho u)_t + (a\rho u^2 + ap)_x = pa_x, \\ a_t = 0. \end{cases} \tag{1.1}$$

where ρ, u, and p represent the density, the velocity and the pressure of the fluid, respectively. The state equation is given by $p = \kappa\rho^\gamma$, where κ is a constant and $1 < \gamma < 3$ for isentropic flow. Generally, $a(x)$ is given a priori, here we view it as a variant which is independent of time [11, 17].

We know that system (1.1) is not conservative because there is a source term which can be seen as a nonconservative product [4, 13]. The source term plays an important role in the numerical approximations both in a nozzle with variable cross-section model and the multiphase flow models [2, 8, 9, 18, 19]. The usual definition of weak solutions cannot be applied to the system. For earlier works on nonconservative systems, see also [5–7].

In 2003, LeFloch et al. [12] solved the Riemann problem of system (1.1). The Riemann problem of nonisentropic fluid was also studied by Andrianov etal. [1] and Thanh [20]. LeFloch and Thanh divided the (u, ρ) plane by the coinciding characteristic curves. In each area, system (1.1) can be viewed as strictly hyperbolic. LeFloch and Thanh select an admissible stationary wave relying on the monotone criterion. While Andrianov et al. give the evolutionary criterion.

In this paper, we study the interaction of the elementary waves including stationary wave, i.e., the interaction of rarefaction wave or shock wave with the stationary wave. The interactions of the elementary waves apart from the stationary wave are obtained by Chang et al. [3]. By using characteristic analysis methods from [3], we study the interactions case by case, based on the solutions of the Riemann problem [1, 12, 20].

*Received: February 12, 2018; Accepted (in revised form): June 8, 2018. Communicated by Alberto Bressan.
This work was supported by NSFC 11371240 and 11771274.
†Department of Mathematics, Shanghai University, Shanghai, China (mathwcsheng@t.shu.edu.cn).
‡Department of Mathematics, Shanghai University, Shanghai, China (zhangqinglong@shu.edu.cn).

2. Preliminaries

2.1. Characteristic analysis and elementary waves. Denoting $U=(u,\rho,a)$, the system (1.1) can be rewritten, when considering a smooth solution, as

$$\partial_t U + A(U)\partial_x U = 0, \tag{2.1}$$

where

$$A=\begin{pmatrix} u & \kappa\gamma\rho^{\gamma-2} & 0 \\ \rho & u & \rho u/a \\ 0 & 0 & 0 \end{pmatrix}.$$

The matrix A has three eigenvalues

$$\lambda_1 = u-c\ ,\ \lambda_2 = 0,\ \lambda_3 = u+c\ , \tag{2.2}$$

where $c=\sqrt{p'(\rho)}$. The corresponding right eigenvectors are

$$\vec{r}_1=(-c,\rho,0)^T\ ,\ \vec{r}_2=\left(-c^2,\rho u, au\left(1-\frac{c^2}{u^2}\right)\right)^T\ ,\ \vec{r}_3=(c,\rho,0)^T.$$

The second characteristic family is linearly degenerate, while the first and the third characteristic families are genuinely nonlinear

$$-\nabla\lambda_1(u)\cdot r_1(u)=\nabla\lambda_3(u)\cdot r_3(u)=\frac{1}{2\sqrt{p'(\rho)}}(\rho p''(\rho)+2p'(\rho))>0.$$

The first and the third characteristics may coincide with the second one, so the system is not strictly hyperbolic. More precisely, setting

$$\Gamma_\pm : u=\pm c,$$

we see that

$$\lambda_2=\lambda_1 \quad \text{on} \quad \Gamma_+, \qquad \lambda_2=\lambda_3 \quad \text{on} \quad \Gamma_-.$$

In the (u,ρ) plane, the curves $\Gamma_\pm$ separate the half-plane $\rho>0$ into three parts. For convenience, we will view them as D_1 (supersonic), D_2 (subsonic) and D_3 (supersonic):

$$D_1=\Big\{(u,\rho)\Big|u<-c\Big\},\quad D_2=\Big\{(u,\rho)\Big||u|<c\Big\},\quad D_3=\Big\{(u,\rho)\Big|u>c\Big\}.$$

In each of the region, the system is strictly hyperbolic and we have

$$\lambda_1<\lambda_3<\lambda_2,\ \text{in } D_1,\quad \lambda_1<\lambda_2<\lambda_3,\ \text{in } D_2,\quad \lambda_2<\lambda_1<\lambda_3,\ \text{in } D_3.$$

For the unsteady flow, we have the Bernoulli's law

$$u^2+\frac{2c^2}{\gamma-1}=k_0, \tag{2.3}$$

where k_0 is constant along a streamline. Furthermore, we have the following result.

LEMMA 2.1. *For unsteady flow, the Bernoulli constant k_0 is constant in the region of flow adjacent to a domain of constant state.*

It follows that the Bernoulli constant k_0 is constant in a simple wave, because a flow in a region adjacent to a region of constant state is always a simple wave.

2.2. The rarefaction waves. First, we look for self-similar solutions. We calculate the Riemann invariants of each characteristic

$$\begin{cases} \lambda_1 = u - c\colon \left\{a, u + \frac{2c}{\gamma-1}\right\}, \\ \lambda_2 = 0\colon \quad \left\{a\rho u, \frac{u^2}{2} + \frac{c^2}{\gamma-1}\right\}, \\ \lambda_3 = u + c\colon \left\{a, u - \frac{2c}{\gamma-1}\right\}. \end{cases} \tag{2.4}$$

We see that, for the rarefaction waves, the cross-section $a(x)$ remains constant, so system (1.1) degenerates to the gas dynamic equations

$$\begin{cases} \rho_t + (\rho u)_x = 0, \\ (\rho u)_t + (\rho u^2 + p)_x = 0. \end{cases} \tag{2.5}$$

For a given left state (u_0, ρ_0, a_0), we determine the 1-wave and 3-wave rarefaction curves that can be connected on the right by

$$\begin{cases} \overleftarrow{R}_1(U, U_0)\colon\ u = u_0 - \displaystyle\int_{\rho_0}^{\rho} \frac{c}{\rho}\,\mathrm{d}\rho = u_0 - \frac{2\sqrt{\kappa\gamma}}{\gamma-1}\left(\rho^{\frac{\gamma-1}{2}} - \rho_0^{\frac{\gamma-1}{2}}\right), & \rho < \rho_0, \\ \overrightarrow{R}_3(U, U_0)\colon\ u = u_0 + \displaystyle\int_{\rho_0}^{\rho} \frac{c}{\rho}\,\mathrm{d}\rho = u_0 + \frac{2\sqrt{\kappa\gamma}}{\gamma-1}\left(\rho^{\frac{\gamma-1}{2}} - \rho_0^{\frac{\gamma-1}{2}}\right), & \rho > \rho_0. \end{cases} \tag{2.6}$$

2.3. The stationary waves. The Rankine-Hugoniot relation associated with the third equation of (1.1) is that

$$-\sigma[a] = 0, \tag{2.7}$$

where $[a] := a_1 - a_0$ is the jump of the cross-section a. We can derive the conclusions:

1) $\sigma = 0$: the shock speed vanishes, here we assume $[a] \neq 0$ and the wave is called stationary contact discontinuity;

2) $[a] = 0$: the cross-section a remains constant across the non-zero speed shocks.

Across the stationary contact discontinuity, the Riemann invariants remain constant; from the second equation of (2.4), the right states (u, ρ, a) satisfy

$$\begin{cases} a_0\rho_0 u_0 = a\rho u, \\ \dfrac{u_0^2}{2} + \dfrac{c_0^2}{\gamma-1} = \dfrac{u^2}{2} + \dfrac{c^2}{\gamma-1}, \end{cases} \tag{2.8}$$

where (u_0, ρ_0, a_0) is the left state. It follows that across the stationary contact discontinuity, the Bernoulli's law is satisfied. We have the following results (see also [12]).

LEMMA 2.2. *Given the left-hand state $U_0 = (u_0, \rho_0, a_0)$ and denote*

$$a_{\min}(U_0) = \frac{a_0\rho_0|u_0|}{\sqrt{\kappa\gamma}\ \bar{\rho}_0^{\frac{\gamma+1}{2}}} \quad \text{and} \quad \bar{\rho}_0 = \left(\frac{2(\gamma-1)}{\kappa\gamma(\gamma+1)}\left(\frac{u_0^2}{2} + \frac{c_0^2}{\gamma-1}\right)\right)^{\frac{1}{\gamma-1}},$$

we have that (2.8) has at most two solutions $U_* = (u_*, \rho_*, a)$ and $U^* = (u^*, \rho^*, a)$ for any $a > 0$, more precisely,

1) if $a < a_{\min}(U_0)$, (2.8) has no solution, so there is no stationary wave.

2) if $a > a_{\min}(U_0)$, there are two points U_*, U^* satisfying (2.8), which can connect with U_0 by stationary waves.

3) if $a=a_{\min}(U_0)$, U_* and U^* coincide.

Proof. We substitute the first equation of (2.8) into the second equation and get

$$-\frac{2\kappa\gamma}{\gamma-1}\rho^{\gamma+1}+\left(u_0^2+\frac{2\kappa\gamma}{\gamma-1}\rho_0^{\gamma-1}\right)\rho^2-\left(\frac{a_0\rho_0u_0}{a}\right)^2=0. \tag{2.9}$$

Let

$$\Phi(\rho;a,U_0)=-\frac{2\kappa\gamma}{\gamma-1}\rho^{\gamma+1}+\left(u_0^2+\frac{2\kappa\gamma}{\gamma-1}\rho_0^{\gamma-1}\right)\rho^2-\left(\frac{a_0\rho_0u_0}{a}\right)^2.$$

From

$$\frac{\mathrm{d}\Phi(\rho;a,U_0)}{\mathrm{d}\rho}=-2\kappa\gamma\frac{\gamma+1}{\gamma-1}\rho^{\gamma}+2\left(u_0^2+\frac{2\kappa\gamma}{\gamma-1}\rho_0^{\gamma-1}\right)\rho=0, \tag{2.10}$$

we get the maximum value of Φ at

$$\bar\rho_0(U_0)=\left(\frac{\gamma-1}{\kappa\gamma(\gamma+1)}u_0^2+\frac{2}{\gamma+1}\rho_0^{\gamma-1}\right)^{\frac{1}{\gamma-1}}=\left(\frac{2(\gamma-1)}{\kappa\gamma(\gamma+1)}\left(\frac{u_0^2}{2}+\frac{c_0^2}{\gamma-1}\right)\right)^{\frac{1}{\gamma-1}}.$$

So Φ has a zero solution at least, as $\Phi(\bar\rho_0;a,U_0)\geqslant 0$. It follows that when

$$a\geqslant\frac{a_0\rho_0|u_0|}{\sqrt{\kappa\gamma}\,\bar\rho_0^{\frac{\gamma+1}{2}}}=:a_{\min}(U_0),$$

$\Phi(\rho;a,u_0)=0$ has a solution at least. If $a\geqslant a_{\mathrm{mim}}(U_0)$, then there exist two values $\rho_*(U_0)\leq\bar\rho_0(U_0)\leq\rho^*(U_0)$ which satisfy

$$\Phi(\rho_*(U_0);a,U_0)=\Phi(\rho^*(U_0);a,U_0)=0. \tag{2.11}$$

We complete the proof of Lemma 2.2. ∎

Moreover, across the stationary contact discontinuity (2.8) denoted by $S_0(U;U_0)$, the states $U_*=(u_*,\rho_*,a)$ and $U^*=(u^*,\rho^*,a)$ have the following properties

$$\begin{cases} S_0(U_*;U_0),\ |u_*|>c_*, & \text{i.e.,}\quad (u_*,\rho_*)\in\begin{cases} D_1,\ u_0<0,\\ D_3,\ u_0>0,\end{cases}\\ S_0(U^*;U_0),\ |u^*|<c^*, & \text{i.e.,}\quad (u_*,\rho_*)\in D_2.\end{cases}$$

As shown in [12], the Riemann problem for (1.1) may admit up to a one-parameter family of solutions. To ensure the uniqueness of the solution, the Riemann solutions should be required to satisfy an Admissibility Criterion: a monotone condition on the component a. Motivated by [1, 12] and [20], we impose the following global entropy condition on stationary wave of (1.1).

Global entropy condition. Along the stationary curve $S_0(U;U_0)$ in the (u,ρ)-plane, the cross-section area a obtained from (2.8) is a monotone function of ρ.

Under the global entropy condition, we call the stationary contact discontinuity as stationary wave in duct flow. Lefloch and Thanh proved the following results in [12].

LEMMA 2.3. *Global entropy condition is equivalent to the statement that any stationary wave has to remain in the closure of only one domain $D_i, i=1,2,3$.*

From the lemma, we get some properties of the stationary curve in (u,ρ)-plane in the following.

LEMMA 2.4. *The stationary wave can be viewed as parameter curves $S_0(U(a);U_0)$ depending only on a in (u,ρ) plane, and they have the following properties*

1) $S_0(U(a);U_0)$ is strictly increasing (decreasing) in u if $u<0$ (>0).

2) $S_0(U(a);U_0)$ is concave with respect to u if $|u|\le c$, or $|u|>c, 2\le\gamma<3$.

3) The increasing (decreasing) velocity and density in U_0 leads to the increasing (decreasing) velocity and density in U.

Proof. Differentiating the two equations of (2.8), we get

$$\begin{cases} \dfrac{\mathrm{d}a}{a}+\dfrac{\mathrm{d}\rho}{\rho}+\dfrac{\mathrm{d}u}{u}=0, \\ u\mathrm{d}u+\kappa\gamma\rho^{\gamma-2}\mathrm{d}\rho=0. \end{cases} \tag{2.12}$$

Then we get

$$\frac{\mathrm{d}\rho}{\mathrm{d}u}=-\frac{u}{\kappa\gamma\rho^{\gamma-2}},\quad \frac{\mathrm{d}u}{\mathrm{d}a}=\frac{uc^2}{a(u^2-c^2)},\quad \frac{\mathrm{d}\rho}{\mathrm{d}a}=-\frac{\rho u^2}{a(u^2-c^2)}.$$

The first statement is hence proved. For the proof of the second statement, we calculate

$$\frac{\mathrm{d}^2\rho}{\mathrm{d}u^2}=-\frac{\rho}{c^4}((\gamma-2)u^2+c^2).$$

From (2.8), we get

$$u=\frac{a_0\rho_0}{a_1\rho}u_0,\quad \rho=\frac{a_0u_0}{a_1u}\rho_0.$$

Taking derivatives with respect to u_0,ρ_0 respectively, when we fix the other variables, we get

$$\frac{\partial u}{\partial u_0}=\frac{a_0\rho}{a_1\rho}>0,\quad \frac{\partial\rho}{\partial\rho_0}=\frac{a_0u_0}{a_1u}>0.$$

Thus the last statement is proved. ∎

From Lemma 2.2 and 2.3, $S_0(U(a);U_0)$ are in the same domain with U_0, see Figure 2.1.

2.4. The shock waves. From (2.7), $a(x)$ remains constant across the shock with non-zero speed, the Rankine-Hugoniot relation for (2.5) is

$$\begin{cases} -\sigma[\rho]+[\rho u]=0, \\ -\sigma[\rho u]+[\rho u^2+p(\rho)]=0, \end{cases} \tag{2.13}$$

which is equivalent to

$$\sigma_i(U,U_0)=u_0\mp\left(\frac{\rho}{\rho_0}\frac{[p]}{[\rho]}\right)^{1/2},\quad i=1,3.$$

The 1-and 3-families of shock waves with non-zero speed connecting a given left-hand state U_0 to the right-hand state U are constrained by the Hugoniot set:

$$(u-u_0)^2=\kappa\left(\frac{1}{\rho_0}-\frac{1}{\rho}\right)(\rho^\gamma-\rho_0^\gamma). \tag{2.14}$$

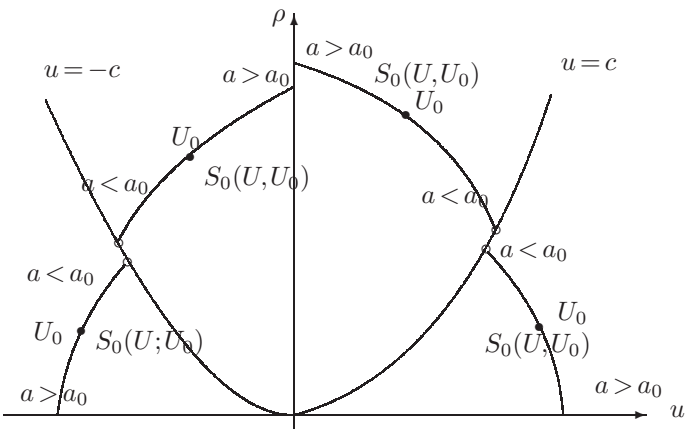

Fig. 2.1. $S_0(U(a),U_0)$ in (u,ρ)-plane.

A shock wave should satisfy the Lax shock conditions [10]

$$\lambda_i(U) < \sigma_i(U,U_0) < \lambda_i(U_0), \quad i=1,3. \tag{2.15}$$

Using the Lax shock conditions, we get the 1- and 3-shock waves $\overleftarrow{S}_1(U,U_0)$ and $\overrightarrow{S}_3(U,U_0)$ consisting of all right-hand states U by

$$\begin{cases} \overleftarrow{S}_1(U,U_0): u = u_0 - \left(\kappa\left(\dfrac{1}{\rho_0}-\dfrac{1}{\rho}\right)(\rho^\gamma-\rho_0^\gamma)\right)^{\frac{1}{2}} & \rho>\rho_0, \\ \overrightarrow{S}_3(U,U_0): u = u_0 - \left(\kappa\left(\dfrac{1}{\rho_0}-\dfrac{1}{\rho}\right)(\rho^\gamma-\rho_0^\gamma)\right)^{\frac{1}{2}} & \rho<\rho_0. \end{cases} \tag{2.16}$$

The 1- and 3-shock wave speeds $\sigma_i(U,U_0)(i=1,3)$ may change their signs along the shock curves in the (u,ρ)-plane, more precisely,

$$\sigma_1(U,U_0) \begin{cases} <0, & U_0 \in D_1 \cup D_2, \\ \left.\begin{array}{l} <0,\ \tilde{\rho}_0<\rho, \\ =0,\ \rho=\tilde{\rho}_0, \\ >0,\ \rho_0<\rho<\tilde{\rho}_0, \end{array}\right\} & U_0 \in D_3, \end{cases} \tag{2.17}$$

and

$$\sigma_3(U,U_0) \begin{cases} >0, & U_0 \in D_2 \cup D_3, \\ \left.\begin{array}{l} >0,\ \bar{\rho}_0<\rho, \\ =0,\ \rho=\bar{\rho}_0, \\ <0,\ \rho_0<\rho<\bar{\rho}_0, \end{array}\right\} & U_0 \in D_1, \end{cases} \tag{2.18}$$

where $\tilde{U}_0=(\tilde{u}_0,\tilde{\rho}_0)\in D_2\cap\{u>0\}, \bar{U}_0=(\bar{u}_0,\bar{\rho}_0)\in D_2\cap\{u<0\}$.

Let us define the backward and forward wave curves

$$W_1(\rho;U_0)=\begin{cases} \overleftarrow{R}_1(\rho;U_0),\ \rho<\rho_0, \\ \overleftarrow{S}_1(\rho;U_0),\ \rho>\rho_0, \end{cases} \qquad W_3(\rho;U_0)=\begin{cases} \overrightarrow{R}_3(\rho;U_0),\ \rho>\rho_0, \\ \overrightarrow{S}_3(\rho;U_0),\ \rho<\rho_0, \end{cases}$$

and stationary wave

$$W_2(\rho;U_0)=S_0(\rho;U_0),\quad \rho=\rho_* \text{ or } \rho^*.$$

We conclude that the wave curve $W_1(\rho;U_0)$ is strictly decreasing and convex in the (u,ρ)-plane, while the wave curve $W_3(\rho;U_0)$ is strictly increasing and convex.

The elementary waves of system (1.1) consists of rarefaction waves, shock waves, and stationary wave, which are denoted by $W_i(\rho;U_0)$ $(i=1,2,3)$ briefly.

According to the Riemann solutions [12] of (1.1) in D_1,D_2, and D_3 , we will consider the interaction results of the elementary waves based on the division of the (u,ρ)-plane. We only consider the interactions of rarefaction waves or shock waves with the stationary waves. The other kinds of wave interactions (rarefaction-rarefaction, shock-shock, shock-rarefaction) can be obtained by the isentropic gas dynamics equations (2.5) [3], using the fact that $[a]=0$ in these cases.

3. The interactions of rarefaction wave or shock wave with the stationary wave

To study the interactions of rarefaction wave or shock wave with the stationary wave, we consider the initial value problem of (1.1) with the initial data

$$(u,\rho,a)\Big|_{t=0}=\begin{cases}U_-=(u_-,\rho_-,a_0), & x<x_1,\\ U_m=(u_m,\rho_m,a_0), & x_1<x<x_2,\\ U_+=(u_+,\rho_+,a_1), & x>x_2.\end{cases}\tag{3.1}$$

3.1. Rarefaction wave interacts with a stationary wave. In this case, it satisfies that

$$U_m\in\overrightarrow{R}_3(U,U_-),\quad U_+\in S_0(U,U_m),\quad a_1\geqslant a_{\min}(U_m).$$

By Lemma 2.1, $a_1\geq a_{\min}(U_0)$ $(\rho_-\leq\rho_0\leq\rho_m)$,$U_0\in\overrightarrow{R}_3(U,U_-)$, which means the stationary wave will always exist in the interaction process. We have that

$$\begin{cases}\overrightarrow{R}_3(U,U_-)=\overrightarrow{R}_3(U_m,U):\ u=u_-+\frac{2\sqrt{\kappa\gamma}}{\gamma-1}(\rho^{\frac{\gamma-1}{2}}-\rho_-^{\frac{\gamma-1}{2}}), & \rho_-\leq\rho\leq\rho_m,\\ S_0(U_1,U_0):\ \begin{cases}a_0\rho_0u_0=a_1\rho_1u_1, & U_0=(u_0,\rho_0,a_0)\in\overrightarrow{R}_3(U,U_-),\\ u_0^2+\dfrac{2\kappa\gamma\rho_0^{\gamma-1}}{\gamma-1}=u_1^2+\dfrac{2\kappa\gamma\rho_1^{\gamma-1}}{\gamma-1}, & a_1\geq a_{\min}.\end{cases}\end{cases}\tag{3.2}$$

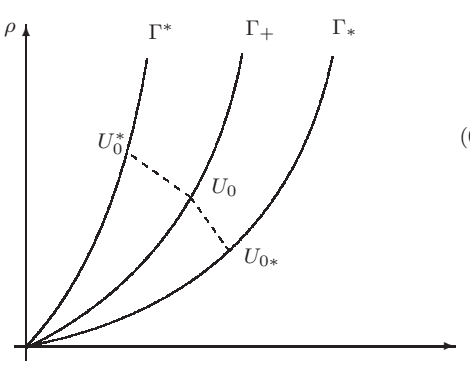

Fig. 3.1. The curves Γ_+,Γ_* and Γ^*.

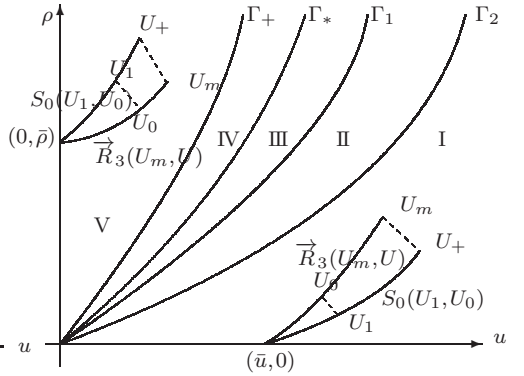

Fig. 3.2. The four curves and the five regions.

Define two curves Γ_* and Γ^* in the (u,ρ)-plane. Γ_* and Γ^* are made of states reached by $S_0(U,U_0)$ using U_{0*} and U_0^* respectively when $U_0\in\Gamma_+$, see Figure 3.1. Then we use the four curves below to divide the (u,ρ)-plane into five parts **I, II, III, IV** and **V**, see Figure 3.2,

$$\Gamma_+:\ u=c,\quad \Gamma_*:\ u=k_0c,\quad \Gamma_1:\ u=k_1c,\quad \Gamma_2:\ u=k_2c,$$

where k_0 is a constant and will be given below, $k_1=\left(\frac{2}{\gamma-1}\right)^{\frac{1}{2}}\left(\frac{a_1}{a_0}\right)^{\frac{\gamma-1}{3-\gamma}}$, $k_2=\frac{2}{\gamma-1}$. Γ_1 will be explained in the following. Γ_2 is the rarefaction curve $\overrightarrow{R}_3(U,(0,0))$, which is below Γ_+. Let $a_1\neq\left(\frac{2}{\gamma-1}\right)^{\frac{3-\gamma}{2(\gamma-1)}}a_0$, then the four curves do not coincide with each other. Without loss of generality, we assume that $a_1<\left(\frac{2}{\gamma-1}\right)^{\frac{3-\gamma}{2(\gamma-1)}}a_0$. We have the following results.

LEMMA 3.1. *$1<k_0<k_1<k_2$, i.e., $\Gamma_+,\Gamma_*,\Gamma_1$ and Γ_2 lie from left to right.*

Proof. The fact that $1<k_1<k_2$ is obvious. We only need to prove $k_0<k_1$.

Let $U_0\in\Gamma_+$, we have $u_0=c_0$. Substituting it into (2.9), we get

$$-\frac{2}{\gamma-1}\left(\frac{\rho}{\rho_0}\right)^{\gamma+1}+\frac{\gamma+1}{\gamma-1}\left(\frac{\rho}{\rho_0}\right)^2-\left(\frac{a_0}{a_1}\right)^2=0,$$

denote $x=\frac{\rho}{\rho_0}$ and $f(x)=-\frac{2}{\gamma-1}x^{\gamma+1}+\frac{\gamma+1}{\gamma-1}x^2-(\frac{a_0}{a_1})^2$, we have $0<x<1$ and

$$f(0)<0,\ f(1)=1-\left(\frac{a_0}{a_1}\right)^2>0,\ f'(x)=\frac{2(\gamma+1)}{\gamma-1}(x-x^\gamma)>0,$$

so $f(x)=0$ admits a unique solution x_0. We substitute $\rho=x_0\rho_0$ into the second equation of (3.2) and get

$$u=\frac{a_0}{a_1}x_0^{-\frac{\gamma+1}{2}}c.$$

Denote $k_0=\frac{a_0}{a_1}x_0^{-\frac{\gamma+1}{2}}$. We know that $k_0<k_1$ if and only if

$$f\left(((\gamma-1)/2)^{\frac{1}{\gamma+1}}(a_0/a_1)^{\frac{4}{(\gamma+1)(3-\gamma)}}\right)<0.$$

The latter follows from the condition $a_1<\left(2/(\gamma-1)\right)^{\frac{3-\gamma}{2(\gamma-1)}}a_0$. The required conclusion follows immediately. ∎

The first quadrant of (u,ρ)-plane can be divided into five parts, namely (see Figure 3.2)

$$\mathrm{I}=\Big\{(u,\rho)\Big|u>k_2c\Big\},\quad \mathrm{II}=\Big\{(u,\rho)\Big|k_1c<u<k_2c\ \Big\},$$
$$\mathrm{III}=\Big\{(u,\rho)\Big|k_0c<u<k_1c\ \Big\},\quad \mathrm{IV}=\Big\{(u,\rho)\Big|c<u<k_0c\ \Big\},\quad \mathrm{V}=\Big\{(u,\rho)\Big|0<u<c\ \Big\}.$$

LEMMA 3.2. *They have the following properties (see Figure 3.2):*

1) If U_+ is above Γ_2, then $\overrightarrow{R}_3(U_m,U_0)$ has a unique intersection point $\overline{U}=(0,\bar{\rho})$ with ρ-axis. And $S_0(U_1,U_0)\cap\overrightarrow{R}_3(U_m,U_0)=\{\overline{U}\}$.

2) If U_+ is below Γ_2, $\overrightarrow{R}_3(U_m,U_0)$ intersects with u-axis at a unique point $\overline{U}=(\bar{u},0)$. And $S_0(U_1,U_0)\cap\overrightarrow{R}_3(U_m,U_0)=\{\overline{U}\}$.

LEMMA 3.3. *The relative position of the curves $S_0(U_1,U_0)$ and $\overrightarrow{R}_3(U_+,U_1)$, when $U_0=U_m$, $U_1=U_+$, is shown as follows*

1) when $U_+\in$ I, $\overrightarrow{R}_3(U_+,U)$ is below (or on the right of) $S_0(U_1,U_0)$ (see Figure 3.3-3.4);

2) when $U_+\in$ II, $S_0(U_1,U_0)$ penetrates $\overrightarrow{R}_3(U_+,U_1)$ from above in the supersonic area, and is above $\overrightarrow{R}_3(U_+,U_1)$ in the subsonic area (see Figure 3.5);

3) when $U_+\in$ III, $S_0(U_1,U_0)$ lies below $\overrightarrow{R}_3(U_+,U_1)$ in the supersonic area, and above $\overrightarrow{R}_3(U_+,U_1)$ in the subsonic area (see Figure 3.6);

4) when $U_+\in$ IV, $\Phi(U_+,U_m)=0$ has no solution.

5) when $U_+\in$ V, $S_0(U_1,U_0)$ is below $\overrightarrow{R}_3(U_+,U_1)$ (see Figure 3.7).

Proof. From the above discussion, we have

$$\begin{cases} U_0=(u_0(\rho_0),\rho_0,a_0)\in\overrightarrow{R}_3(U_m,U): u=u_m+\dfrac{2\sqrt{\kappa\gamma}}{\gamma-1}(\rho^{\frac{\gamma-1}{2}}-\rho_m^{\frac{\gamma-1}{2}}), \quad 0\le\rho\le\rho_m, \\ U_1=(u_1(\rho_1),\rho_1,a_1)\in S_0(U,U_0): \begin{cases} a_0\rho_0u_0=a_1\rho u, \\ u_0^2+\dfrac{2\kappa\gamma\rho_0^{\gamma-1}}{\gamma-1}=u^2+\dfrac{2\kappa\gamma\rho^{\gamma-1}}{\gamma-1}, \end{cases} 0\le\rho\le\rho_+, \end{cases} \tag{3.3}$$

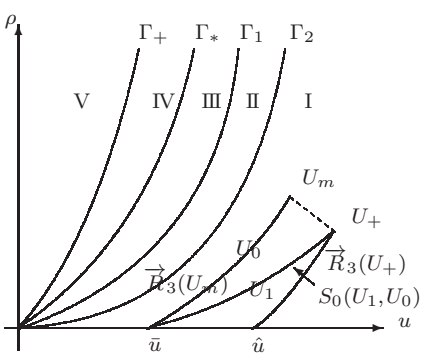

Fig. 3.3. $U_+\in$ I and U_m is below Γ_2.

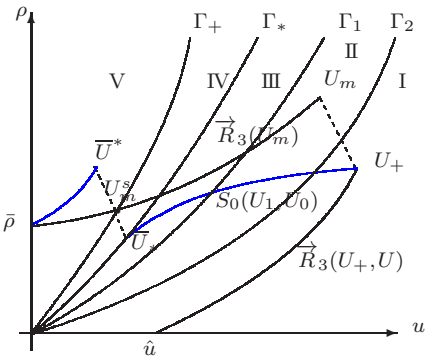

Fig. 3.4. $U_+\in$ I and U_m is above Γ_2.

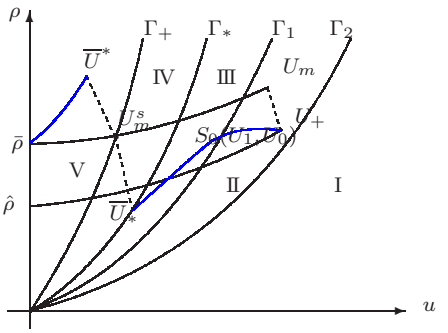

Fig. 3.5. $U_+ \in \mathrm{II}$.

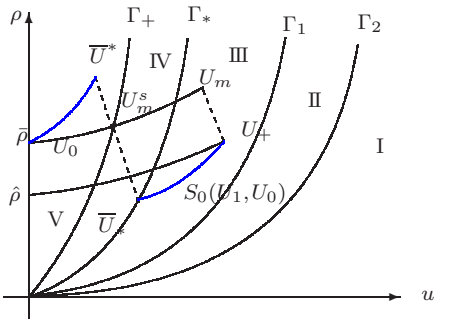

Fig. 3.6. $U_+ \in \mathrm{III}$.

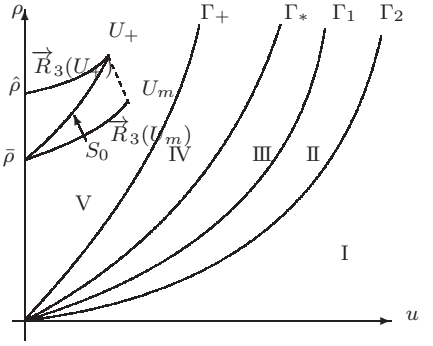

Fig. 3.7. $U_+ \in \mathrm{V}$.

and

$$\overrightarrow{R}_3(U_+,U):\quad u=u(\rho)=u_+ + \frac{2\sqrt{\kappa\gamma}}{\gamma-1}(\rho^{\frac{\gamma-1}{2}}-\rho_+^{\frac{\gamma-1}{2}}),\quad 0\le\rho\le\rho_+. \tag{3.4}$$

Denote $f(\rho_1)=u_1(\rho_1)-u(\rho_1)$, when U_+ is located below Γ_+. Then we have $f(\rho_+)=0$. From (3.3), we have

$$\begin{cases} \mathrm{d}u_0=\sqrt{\kappa\gamma}\rho_0^{\frac{\gamma-3}{2}}\mathrm{d}\rho_0, \\ a_0\rho_0\mathrm{d}u_0+a_0u_0\mathrm{d}\rho_0=a_1\rho_1\mathrm{d}u_1+a_1u_1\mathrm{d}\rho_1, \\ u_0\mathrm{d}u_0+\kappa\gamma\rho_0^{\gamma-2}\mathrm{d}\rho_0=u_1\mathrm{d}u_1+\kappa\gamma\rho_1^{\gamma-2}\mathrm{d}\rho_1. \end{cases} \tag{3.5}$$

It follows that

$$\frac{\mathrm{d}u_1}{\mathrm{d}\rho_1}=\frac{a_1u_1\sqrt{\kappa\gamma}-a_0\kappa\gamma\rho_0^{-\frac{\gamma-3}{2}}\rho_1^{\gamma-2}}{a_0\rho_0^{-\frac{\gamma-3}{2}}u_1-a_1\rho_1\sqrt{\kappa\gamma}}. \tag{3.6}$$

Therefore, we get that

$$\begin{aligned}\frac{\mathrm{d}f}{\mathrm{d}\rho_1}&=\frac{\mathrm{d}u_1}{\mathrm{d}\rho_1}-\frac{\mathrm{d}u}{\mathrm{d}\rho_1}=\frac{a_1u_1\sqrt{\kappa\gamma}-a_0\kappa\gamma\rho_0^{-\frac{\gamma-3}{2}}\rho_1^{\gamma-2}}{a_0\rho_0^{-\frac{\gamma-3}{2}}u_1-a_1\rho_1\sqrt{\kappa\gamma}}-\sqrt{\kappa\gamma}\rho_1^{\frac{\gamma-3}{2}}\\ &=-\frac{u_1+c_1}{\rho_1}\cdot\frac{u_1c_1-u_0c_0}{u_1^2-u_0c_0}.\end{aligned} \tag{3.7}$$

Similarly, denote $g(u_1)=\rho_1(u_1)-\rho(u_1)$, we have $g(u_+)=0$ and

$$\frac{\mathrm{d}g}{\mathrm{d}u_1}=\frac{\rho_1(u_1+c_1)(u_1c_1-u_0c_0)}{u_1c_1(u_0c_0-c_1^2)}.$$

Firstly, we have

$$u_1^2-u_0c_0\ \begin{cases}>0 & U_1\in\mathrm{I}\cup\mathrm{II}\cup\mathrm{III},\\ <0 & U_1\in\mathrm{V},\end{cases}\quad\text{and}\quad u_0c_0-c_1^2\ \begin{cases}>0 & U_1\in\mathrm{I}\cup\mathrm{II}\cup\mathrm{III},\\ <0 & U_1\in\mathrm{V}.\end{cases}$$

Secondly, we know that

$$u_1c_1-u_0c_0=u_0c_0\left(\frac{u_1c_1}{u_0c_0}-1\right)=u_0c_0\left(\frac{u_1}{u_0}\cdot\left(\frac{\rho_1}{\rho_0}\right)^{\frac{\gamma-1}{2}}-1\right)=u_0c_0\left(\frac{a_0}{a_1}\cdot\left(\frac{\rho_0}{\rho_1}\right)^{\frac{3-\gamma}{2}}-1\right).$$

Thus from $u_1c_1=u_0c_0$, we have

$$\frac{a_0}{a_1}=\left(\frac{\rho_0}{\rho_1}\right)^{\frac{\gamma-3}{2}}. \tag{3.8}$$

and substitute (3.8) into (2.9) :

$$u_1^2=\frac{2}{\gamma-1}\left(\frac{a_1}{a_0}\right)^{\frac{2(\gamma-1)}{3-\gamma}}c_1^2.$$

Denote $k_1=\left(\frac{2}{\gamma-1}\right)^{\frac{1}{2}}\left(\frac{a_1}{a_0}\right)^{\frac{\gamma-1}{3-\gamma}}$, $a_*=\left(\frac{2}{\gamma-1}\right)^{\frac{3-\gamma}{2(\gamma-1)}}a_0$, thus we obtain the curve Γ_1.

When $a_1<a_*$, Γ_1 lies between Γ_+ and Γ_2. While $a_1>a_*$, Γ_+ lies between Γ_1 and Γ_2. We only consider the case $a_1<a_*$. The other case is similar.

Combining the above discussion, we have

$$u_1c_1-u_0c_0\ \begin{cases}<0,\ U_1\in\mathrm{I}\cup\mathrm{II},\\ >0,\ U_1\in\mathrm{III},\\ <0,\ U_1\in\mathrm{V}.\end{cases}$$

Therefore,

$$\frac{\mathrm{d}f}{\mathrm{d}\rho_1}\ \begin{cases}>0, & U_1\in\mathrm{I}\cup\mathrm{II},\\ <0, & U_1\in\mathrm{III}\cup\mathrm{V},\end{cases}\quad\text{and}\quad\frac{\mathrm{d}g}{\mathrm{d}u_1}\ \begin{cases}<0, & U_1\in\mathrm{I}\cup\mathrm{II},\\ >0, & U_1\in\mathrm{III}\cup\mathrm{V}.\end{cases} \tag{3.9}$$

(1) $U_+\in\mathrm{I}$, the location of U_m has two subcases:

1) U_m is below Γ_2, $S_0(U_1,U_0)$ interacts with u-axis at $(\bar{u},0)$, since $f'(\rho_1)>0$, and $f(\rho_+)=0$, so $f(\rho_1)<0$ when $0\le\rho_1\le\rho_+$, thus $S_0(U_1,U_0)$ is on the left of $\overrightarrow{R}_3(U_+,U_1)$. See Figure 3.3.

2) U_m is above Γ_2. Denote $U_m^s=(u_m^s,\rho_m^s)=\overrightarrow{R}_3(U_m,U)\cap\Gamma_+$, $S_0(U,U_m)$ jumps from $\overline{U}_*=(\overline{u}_*,\overline{\rho}_*)$ below Γ_+ to $\overline{U}^*=(\overline{u}^*,\overline{\rho}^*)$ above Γ_+. This case indicates that $S_0(U_1,U_0)$ will penetrate through Γ_2 and stay above Γ_2 since the sign of $\frac{\mathrm{d}g}{\mathrm{d}u_1}$ changes only once when $U_+\in\mathrm{I}\cup\mathrm{II}\cup\mathrm{III}$. Therefore, $S_0(U_1,U_0)$ lies above $\overrightarrow{R}_3(U_+,U_1)$ both in the supersonic and subsonic areas. See Figure 3.4.

(2) $U_+ \in \mathrm{II}$, U_m in $\mathrm{II} \cup \mathrm{III}$, since $\frac{\mathrm{d}g}{\mathrm{d}u_1} < 0$ ($U_1 \in \mathrm{II}$) and $\frac{\mathrm{d}g}{\mathrm{d}u_1} > 0$ ($U_1 \in \mathrm{III}$). In the supersonic area, $S_0(U_1,U_0)$ is above $\overrightarrow{R}_3(U_+,U_1)$ at first, intersects with $\overrightarrow{R}_3(U_+,U_1)$ and then reaches $\overline{U}_*$ below $\overrightarrow{R}_3(U_+,U_1)$. See Figure 3.5.

(3) $U_+ \in \mathrm{III}$, then $U_m \in \mathrm{III} \cup \mathrm{IV}$. In this case $\frac{\mathrm{d}g}{\mathrm{d}u_1} > 0$. $g(u_+) = 0$, so $g(u_1) < 0$ when $\overline{u}_* \le u_1 \le u_+$. $S_0(U_1,U_0)$ is below $\overrightarrow{R}_3(U_+,U_1)$ in the supersonic area. See Figure 3.6.

(4) $U_+ \in \mathrm{IV}$. Obviously.

(5) $U_+ \in \mathrm{V}$. Similarly, $g(u_1) < 0$ when $0 \le u_1 \le u_+$. $S_0(U_1,U_0)$ is below $\overrightarrow{R}_3(U_+,U_1)$. See Figure 3.7.

□

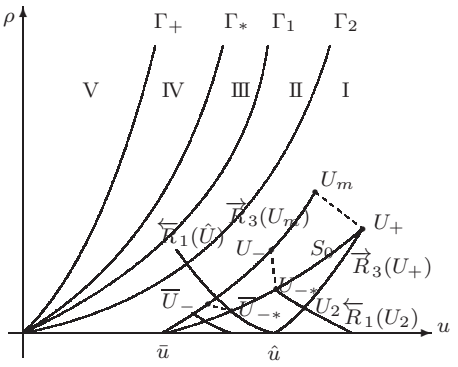

Fig. 3.8. Case 1. $U_+ = (u_+,\rho_+) \in \mathrm{I}$.

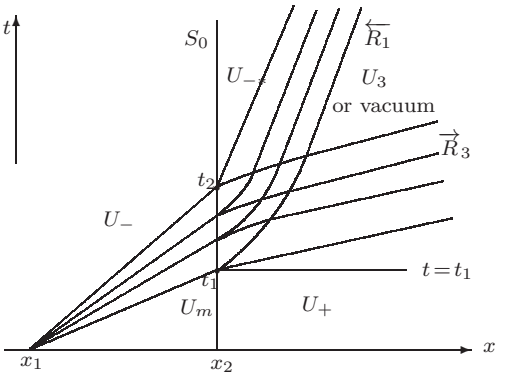

Fig. 3.9. The solutions for case 1.1.

Next, we will discuss the interactions case by case.

Case 1. $U_+ = (u_+,\rho_+) \in \mathrm{I}$, U_m is below Γ_2. See Figure 3.8.

In this case, from the result 1) in Lemma 3.3, we draw curves $\overrightarrow{R}_3(U_+,U)$, $\overrightarrow{R}_3(U_m,U)$, $S_0(U_1,U_0)$ starting from U_+, and $\overleftarrow{R}_1(\hat{U},U)$ passing through $\hat{U} = (\hat{u},0) \in \overrightarrow{R}_3(U_+,U)$. Denote the intersection point of $S_0(U_1,U_0)$ and $\overleftarrow{R}_1(\hat{U})$ ($\hat{U}$ is the right-hand state) as $\overline{U}_{-*}$, which is obtained by $U_0 = \overline{U}_- \in \overrightarrow{R}_3(U_m,U)$.

Case 1.1. U_- is between U_m and $\overline{U}_-$ on the curve $\overrightarrow{R}_3(U_m,U)$.

We solve the initial boundary value problem (2.5) with

$$(u,\rho) = \begin{cases} (u_+,\rho_+), & t = t_1, x > x_2, \\ (u_1,\rho_1), & t_1 < t < t_2, x = x_2, \\ (u_{-*},\rho_{-*}), & t \ge t_2, x = x_2, \end{cases} \tag{3.10}$$

in the domain $\{(x,t) \big| x \ge x_2, t \ge t_1\}$, where $(u_1,\rho_1) \in S_0(U_1,U_0)$, $U_0 \in \overrightarrow{R}_3(U_m,U)$.

Because on the boundary $S_0 : t > t_1, x = x_2 + 0, \lambda_{1,3} = u_1 \pm c_1 > 0$, there exists a unique solution in the domain from the theory of the isentropic gas dynamical system. Finally, the large-time behavior of the solution is

$$U_- \oplus S_0(U_{-*},U_-) \oplus \overleftarrow{R}_1(U_2,U_{-*}) \oplus \overrightarrow{R}_3(U_+,U_2) \oplus U_+,$$

where "$\oplus$" means "follows". The result is shown as in Figure 3.9.

Case 1.2. U_- is below $\overline{U}_-$ on the curve $\overrightarrow{R}_3(U_m,U)$. In this case, U_2 turns to vacuum. See Figure 3.9.

Case 2. $U_+=(u_+,\rho_+)\in \mathrm{I}$, U_m is above Γ_2. See Figure 3.10.

Subcase 2.1. As $U_-\notin \mathrm{V}$, which is on $\overrightarrow{R}_3(U_m,U)$ and in the supersonic area, it is similar to the Case 1.1. We omit it. See Figure 3.9-3.10.

Subcase 2.2. As $U_-\in \mathrm{V}$, which is in the subsonic area and below U_m^s both on $\overrightarrow{R}_3(U_m,U)$. $S_0(U_1,U_0)$ touches Γ_* at $\overline{U}_*$ and coincides with $\widehat{O\overline{U}_*}$ on Γ_* in the supersonic area. The interaction starts at time $t=t_1$. The process of interaction includes two parts. In the first part from t_1 to t_2,$U_0\in\overrightarrow{R}_3(U,U_-)$ (U_0 is between U_m and U_m^s), $U_1\in S_0(U_1,U_0)$ (U_1 is between U_+ and $\overline{U}_*$). This process is the same as the above case. In the second part from t_2 to t_3, $U_0\in\Gamma_+\cap\overleftarrow{R}_1(U,\overline{U}_m)$ ($\overline{U}_m\in\overrightarrow{R}_3(U_m,U)$ is between U_m^s and U_-), $U_1\in S_0(U_1,U_0)$ (U_1 is between $\overline{U}_*$ and U_{2*}). We need to solve the initial boundary value problems of (2.5) on the left-side of $x=x_2$ with

$$(u,\rho)=\begin{cases}\left(\dfrac{\gamma-1}{\gamma+1}\left(u_--\dfrac{2c_-}{\gamma-1}+\dfrac{2\xi}{\gamma-1}\right),\left(\dfrac{(\xi-u)^2}{\kappa\gamma}\right)^{\frac{1}{\gamma-1}}\right), & (x,t)\in C_-,u_--c_-<\xi<u_m-c_m,\\ u=c, & t_2<t<t_3,x=x_2,\\ (u_2,\rho_2), & t>t_3,x=x_2,\end{cases}\tag{3.11}$$

and on the right-side of $x=x_2$ with

$$(u,\rho)=\begin{cases}(u_+,\rho_+), & t=t_1,x>x_2,\\ (u_1,\rho_1), & t_1<t<t_2,x=x_2,\\ u=k_0c, & t_2<t<t_3,x=x_2,\\ x=x_2, & \end{cases}\tag{3.12}$$

respectively, where ξ is the given slope of the characteristic lines of $\overleftarrow{R}_1(U_m,U_-)$, C_- is denoted as the penetrating backward characteristic, see Figure 3.11, k_0 is given in Lemma 3.1. The existence and uniqueness of the two problems can be obtained by the classical theory from Li et al. [14] and Wang et al. [21]. The solutions are shown in Figure 3.11.

Furthermore, we get the large-time behavior of the solution from the theory of isentropic gas dynamical system (2.5) as

$$U_-\oplus\overleftarrow{R}_1(U_2,U_-)\oplus S_0(U_{2*},U_2)\oplus\overleftarrow{R}_1(U_3,U_{2*})\oplus\overrightarrow{R}_3(U_+,U_3)\oplus U_+.$$

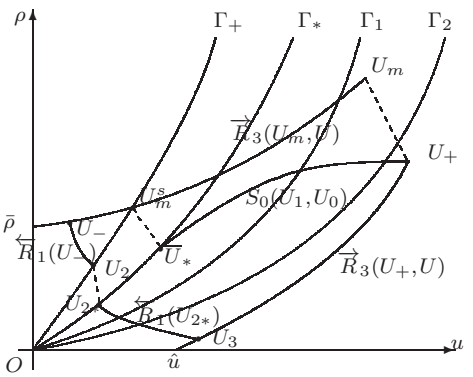

Fig. 3.10. Case 2. U_- is below $\overline{U}_-$.

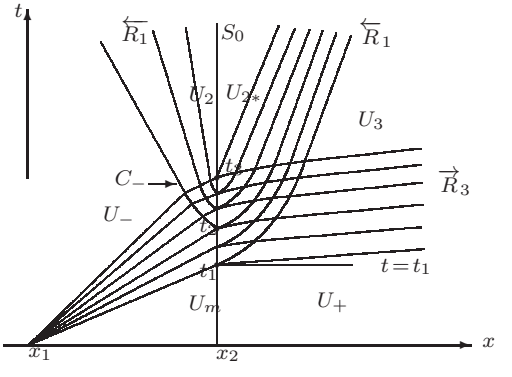

Fig. 3.11. The solutions for subcase 2.2.

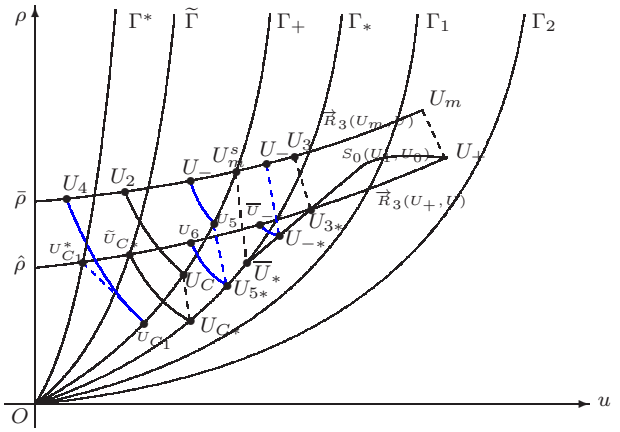

Fig. 3.12. Case 3. $(u_+,\rho_+)\in \mathrm{II}$.

Case 3. $U_+=(u_+,\rho_+)\in \mathrm{II}$. See Figure 3.12.

By 2) in Lemma 3.3, $S_0(U_1,U_0)$ penetrates $\overrightarrow{R}_3(U_+,U)$ from above, intersects with $\overrightarrow{R}_3(U_+,U)$ at U_{3*}, which is obtained by $S_0(U_3,U_{3*})$ $(U_3\in\overrightarrow{R}_3(U_m,U))$, touches Γ_* at $\overline{U}_*$, and coincides with $\widehat{O\overline{U}_*}$ on Γ_* in the supersonic area.

By virtue of (2.17), from any point $U\in\Gamma_*$, there exists a point $\widetilde{U}\in D_2$ such that the 1-shock speed from U to $\widetilde{U}$ vanishes, i.e., $\sigma_1(\widetilde{U},U)=0$. Such states $\widetilde{U}$ form a curve in D_2, denoted by $\widetilde{\Gamma}$, see Figure 3.12. $\widetilde{\Gamma}$ is determined by

$$\begin{cases}\rho u=\tilde{\rho}\tilde{u},\\ \rho u^2+p(\rho)=\tilde{\rho}\tilde{u}^2+p(\tilde{\rho}),\end{cases}\qquad U=(u,\rho)\in\Gamma_*. \tag{3.13}$$

We will show that $\widetilde{\Gamma}$ and $\overrightarrow{R}_3(U_+,U)$ have only one intersection point. On Γ_*, $u=k_0c$, where $k_0>1$ is given in Lemma 3.1. Substituting it into (3.13), we have

$$k_0^2\gamma\rho^{\gamma+1}+\tilde{\rho}^{\gamma+1}-(k_0^2\gamma+1)\rho^\gamma\tilde{\rho}=0,$$

where $\tilde{\rho}>\rho$. By a similar calculation as in Lemma 3.1, we obtain that there exists a constant $\tilde{k}_0$, $0<\tilde{k}_0<1$, such that $\tilde{u}=\tilde{k}_0\tilde{c}$. Denote the two curves $\widetilde{\Gamma}$ and $\overrightarrow{R}_3(U_+,U)$ as $\tilde{\rho}=\tilde{\rho}(u)$ and $\rho=\rho(u)$ respectively, and $\tilde{f}(u)=\tilde{\rho}(u)-\rho(u)$. Firstly, from $\tilde{f}(0)=\tilde{\rho}(0)-\rho(0)=-\hat{\rho}<0$, $\tilde{f}(+\infty)>0$, we conclude that the two curves have at least one intersection. Secondly, a direct calculation shows that $\mathrm{d}\tilde{f}/\mathrm{d}u>0$. It follows that the intersection point is unique, which is denoted by $\widetilde{U}_{C*}$.

Denote $U^*_{C_1}=\overrightarrow{R}_3(U_+,U)\cap\Gamma^*$, which is obtained by $U_{C_1}\in\Gamma_+$. We find a point $U_4\in\overrightarrow{R}_3(U_m,U)$, which is connected with U_{C_1} by $\overleftarrow{R}_1(U_{C_1},U_4)$. Denote $U_{C*}\in\Gamma_*$, which is obtained by a zero-speed shock $\overleftarrow{S}_1(\widetilde{U}_{C*},U_{C*})$: $\sigma_1(\widetilde{U}_{C*},U_{C*})=0$. U_{C*} connects with $U_C\in\Gamma_+$ by a stationary wave $S_0(U_{C*},U_C)$, denote $U_2=\overleftarrow{R}_1(U_C,U)\cap\overrightarrow{R}_3(U_m,U)$. By (2.17), we know that U_2 is a critical point. When U is above U_{C*} on Γ_*, it gets to a point $\overline{U}$ on $\overrightarrow{R}_3(U_+,U)$ by a shock wave with positive speed $\sigma_1(\overline{U},U)>0$. When U is below U_{C*} on Γ_*, it gets to a point $\overline{U}$ on $\overrightarrow{R}_3(U_+,U)$ by a shock wave with negative speed $\sigma_1(\overline{U},U)<0$.

Subcase 3.1. U_- is between U_m and U_3 on the curve $\overrightarrow{R}_3(U_m,U)$ (Figure 3.12), it is similar to Case 1.1. See Figure 3.9.

Subcase 3.2. U_- is between U_3 and U_m^s on the curve $\overrightarrow{R}_3(U_m,U)$ (Figure 3.12). The interaction includes two parts, the first part from time t_1 to t_2, $U_0\in\overrightarrow{R}_3(U,U_-)$ (U_0 is between U_m and U_3), $U_1\in S_0(U_1,U_0)$ (U_1 is between U_+ and U_{3*}). This process is similar to the Case 1.1, we get the solution in Figure 3.13 (right). Figure 3.13 (left) shows the critical case that $U_-=U_3$. In this case $(u,\rho)=U_{3*}=(u_{3*},\rho_{3*})\in S_0(U_{3*},U_3)$ in the domain $\{x<x_2+(u_{3*}+c_{3*})(t-t_2)\big|t>t_2\}$.

In the second part from t_2 to t_3, where U_0 is between U_3 and U_- on the curve $\overrightarrow{R}_3(U_m,U)$, $U_1\in S_0(U_1,U_0)$ (U_1 is between U_{3*} and U_{-*}), we solve the free boundary value problem

$$\begin{cases}\begin{cases}\dfrac{\mathrm{d}x}{\mathrm{d}t}=u_l-\left(\dfrac{\rho_r(p(\rho_r)-p(\rho_l))}{\rho_l(\rho_r-\rho_l)}\right)^{\frac12},\\ u_r=u_l-\left(\kappa\left(\dfrac{1}{\rho_l}-\dfrac{1}{\rho_r}\right)(\rho_r^\gamma-\rho_l^\gamma)\right)^{\frac12}, \qquad (\text{the Rankine}-\text{Hugoniot condition of } \overleftarrow{S}_1)\\ x(t_2)=x_2,\end{cases}\\ \mathrm{d}u_l=\sqrt{\kappa\gamma}\rho_l^{\frac{\gamma-3}{2}}\mathrm{d}\rho_l,\ \rho_{-*}<\rho_l<\rho_{3*}, \qquad (U_l\in\overrightarrow{R}_3(U,U_{-*}) \text{ on the left side of } \overleftarrow{S}_1)\\ \mathrm{d}u_r=\sqrt{\kappa\gamma}\rho_r^{\frac{\gamma-3}{2}}\mathrm{d}\rho_r,\ \overline{\rho}_{-*}<\rho_r<\rho_{3*}, \qquad (U_r\in\overrightarrow{R}_3(U,\overline{U}_{-*}) \text{ on the right side of } \overleftarrow{S}_1)\\ (u,\rho)=\begin{cases}(u_{3*},\rho_{3*}), & \frac{x-x_2}{t-t_2}=u_{3*}+c_{3*},x>x_2,\\ (u_1,\rho_1), & t_2<t<t_3,x=x_2,\\ (u_{-*},\rho_{-*}), & t>t_3,x=x_2.\end{cases}\end{cases} \tag{3.14}$$

where $p(\rho_l)=\kappa\rho_l^\gamma,p(\rho_r)=\kappa\rho_r^\gamma$ and $x=x(t)$ is the shock wave supplemented by the Lax entropy condition: $0<u_r-c_r<\dfrac{\mathrm{dx}}{\mathrm{dt}}<u_l-c_l$. So the shock wave $\overleftarrow{S}_1$ propagates with positive speed in the domain, from [3], we know that the speed of $\overleftarrow{S}_1$ will be decreasing during the process of penetrating $\overrightarrow{R}_3$, see Figure 3.13 (right). Furthermore, the large-time behavior of the solution from the theory of isentropic gas dynamic system (2.5) is given as

$$U_-\oplus S_0(U_{-*},U_-)\oplus\overleftarrow{S}_1(\overline{U}_{-*},U_{-*})\oplus\overrightarrow{R}_3(U_+,\overline{U}_{-*})\oplus U_+.$$

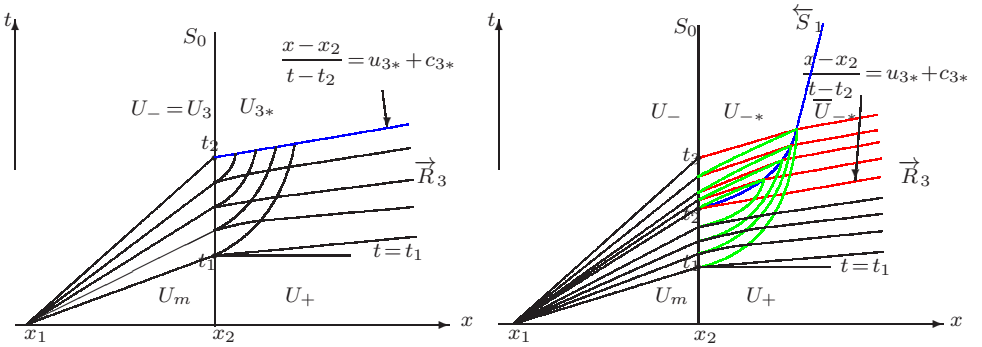

Fig. 3.13. The solutions for subcase 3.2.

Subcase 3.3. U_- is between U_m^s and U_2 on the curve $\overrightarrow{R}_3(U_m,U)$ (Figure 3.12). The interaction includes three parts, the first part is from time t_1 to t_2, where $U_0\in\overrightarrow{R}_3(U,U_-)$ (U_0 is between U_m and U_3), and the second part is from time t_2 to t_3, where $U_0\in$

$\overrightarrow{R}_3(U,U_-)$ (U_0 is between U_3 and U_m^s). Both the above parts are the same as subcase 3.2, which we have discussed. The third part is from t_3 to t_4, where $U_0 \in \Gamma_+ \cap \overleftarrow{R}_1(U,\overline{U}_m)$ ($\overline{U}_m$ is between U_m^s and U_-), $U_1 \in S_0(U_1,U_0)$ (U_1 is between U_{5*} and $\overline{U}_*$). A backward rarefaction wave reflects in this part and coincides with S_0, which is similar to the subcase 2.2. At the critical case $U_- = U_2$, we have $U_0 = U_C, U_1 = U_{C*}$, the speed equals to zero in this case. Similarly, we get the solution by solving initial (free) boundary value problems as (3.10), (3.11) and (3.14), see Figure 3.14. The large-time behavior of the solution from the theory of isentropic gas dynamical system (2.5) is

$$U_- \oplus \overleftarrow{R}_1(U_5,U_-) \oplus S_0(U_{5*},U_5) \oplus \overleftarrow{S}_1(U_6,U_{5*}) \oplus \overrightarrow{R}_3(U_+,U_6) \oplus U_+.$$

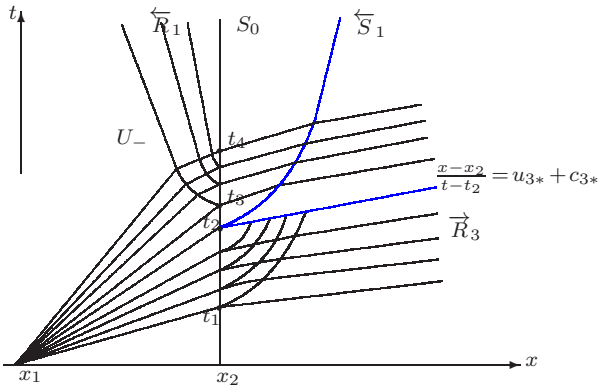

Fig. 3.14. The solutions for subcase 3.3.

Subcase 3.4. U_- is between U_2 and U_4 on the curve $\overrightarrow{R}_3(U_m,U)$ (Figure 3.12). The interaction includes four parts. The first three parts from time t_1 to t_4 are the same as subcase 3.3. A shock wave $\overleftarrow{S}_1$ with positive speed transmits during the interaction process, see Figure 3.15-2. When U_0 goes down along Γ_+ passing U_C, the speed of $\overleftarrow{S}_1$ decreases in $\overrightarrow{R}_3$ as $t \geq t_2$ by (2.17). At the critical case $U_0 = U_C$, the speed of $\overleftarrow{S}_1$ equals to zero and becomes negative when U_0 is below U_C on the curve Γ_+. It keeps a constant negative speed after penetrating $\overrightarrow{R}_3$.

The fourth part is from t_4 to t_5. $\overleftarrow{S}_1$ penetrates $\overrightarrow{R}_3$ and touches S_0 at $t = t_5$ during this period. Figure 3.15-1 shows the transition between subcase 3.3 and 3.4. On the one hand, U_- connects with U_A on Γ_+ through $\overleftarrow{R}_1(U_A,U_-)$, U_A jumps to U_{A*} by S_0, and U_{A*} gets to U_8 on $\overrightarrow{R}_3(U_+,U)$ by a backward shock wave with negative speed: $\sigma_1(U_8,U_{A*}) < 0$. On the other hand, we solve a generalized Riemann problem at time $t = t_5$. The solution includes backward waves $\overleftarrow{R}_1$ and $\overleftarrow{S}_1$, which connects U_- and U_7. U_7 jumps to U_7^* by stationary wave, and U_7^* connects with U_8 by a forward shock wave. Here, U_7, U_7^* and U_8 are determined by

$$\begin{cases} \dfrac{\mathrm{d}x}{\mathrm{d}t} = u_l - \left(\dfrac{\rho_7(p(\rho_7) - p(\rho_l))}{\rho_l(\rho_7 - \rho_l)} \right)^{\frac{1}{2}}, \\ u_7 = u_l - \left(\kappa \left(\dfrac{1}{\rho_l} - \dfrac{1}{\rho_7} \right) (\rho_7^\gamma - \rho_l^\gamma) \right)^{\frac{1}{2}}, \quad \text{(the R}-\text{H condition of } \overleftarrow{S}_1(U_7,U_l)) \\ x(t_5) = x_2, \end{cases} \tag{3.15}$$

and

$$\begin{cases} \mathrm{d}u_l = \sqrt{\kappa\gamma}\rho_l^{\frac{\gamma-3}{2}}\mathrm{d}\rho_l,\ \rho_A<\rho_l<\rho_7, & (U_l\in \overrightarrow{R}_3(U,U_-) \text{ on the left side of } \overleftarrow{S}_1)\\ \begin{cases} a_0\rho_7 u_7 = a_1\rho_7^* u_7^*,\\ \dfrac{u_7^2}{2}+\dfrac{c_7^2}{\gamma-1}=\dfrac{u_7^{*2}}{2}+\dfrac{c_7^{*2}}{\gamma-1}, \end{cases} & (U_7,\ U_7^* \text{ are connected by } S_0(U_7^*,U_7))\\ \begin{cases} u_7^* = u_8+\left(\kappa\left(\dfrac{1}{\rho_7^*}-\dfrac{1}{\rho_8}\right)\left(\rho_8^\gamma-\rho_7^{*\gamma}\right)\right)^{\frac{1}{2}},\\ \rho_8<\rho_7^*, \end{cases} & (\text{the R}-\text{H condition of } \overrightarrow{S}_3(U_8,U_7^*)). \end{cases} \tag{3.16}$$

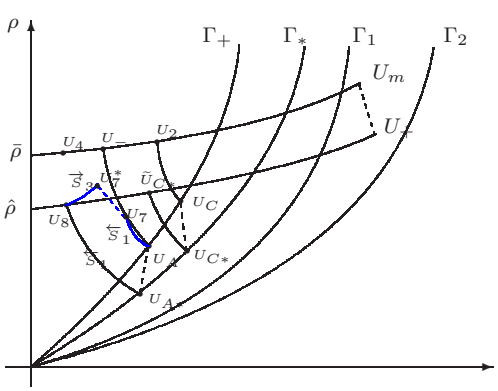

Fig. 3.15-1. The transition between subcase 3.3-3.4.

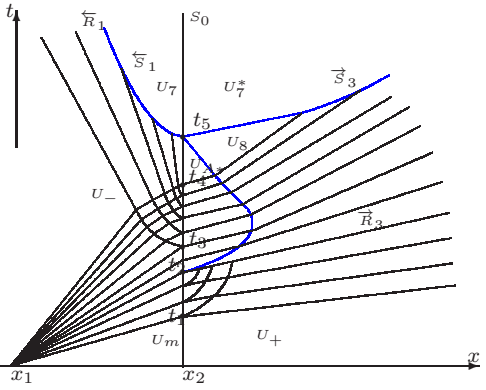

Fig. 3.15-2. The solutions for subcase 3.4.

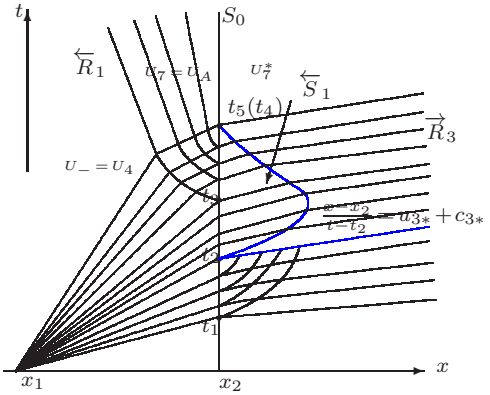

Fig. 3.15-3. The critical case $U_- = U_4$.

There exists a unique solution of (3.15) by using the phase plane analysis method, see Figure 3.15-1. The shock wave $\overleftarrow{S}_1$ interacts with $\overleftarrow{R}_1$ and leaves $\overleftarrow{R}_1$ on the left of S_0 when $t\to+\infty$. On the right of S_0, $\overrightarrow{S}_3$ will interact with $\overrightarrow{R}_3$, a direct calculation shows that $\overrightarrow{S}_3$ does not cross $\overrightarrow{R}_3$ completely, see Figure 3.15-2.

When U_- is close to U_4, the speed of both $\overleftarrow{S}_1$ and $\overrightarrow{S}_3$ will decrease. At the critical case $U_- = U_4$, t_4 and t_5 coincide. We have $U_7 = U_A = U_{C_1}$, $U_7^* = U_8 = U_{C_1}^*$; in this case, so there are no shock waves emitted when $t > t_5$. See Figure 3.15-3.

Subcase 3.5. U_- is between U_4 and $\bar{U} = (0,\bar{\rho})$ on the curve $\overrightarrow{R}_3(U_m,U)$ (Figure 3.12).

The interaction includes four parts, the first three parts from t_1 to $t_4(t_5)$ are the same with subcase 3.5. The fourth part is from t_5 to t_6. At the time $t=t_5$, we solve a generalized Riemann problem. The solution includes a forward rarefaction wave $\overrightarrow{R}_3$ connecting U_9 and $U^*_{C_1}$ on the right side of S_0, see Figure 3.16 (left). On the left side of S_0, we solve the initial boundary value problem of isentropic gas dynamical system with

$$(u,\rho)=\begin{cases}\left(\dfrac{\gamma-1}{\gamma+1}\left(u_- -\dfrac{2c_-}{\gamma-1}+\dfrac{2\xi}{\gamma-1}\right),\dfrac{(\xi-u)^{\frac{2}{\gamma-1}}}{(\kappa\gamma)^{\frac{1}{\gamma-1}}}\right), & (x,t)\in C_-, u_- -c_- <\xi< u^s_m-c^s_m,\\ u=c, & t_3<t<t_5, x=x_2,\\ U=U_0, & t_5<t<t_6, x=x_2,\\ (u_9,\rho_9), & t>t_6, x=x_2,\end{cases} \tag{3.17}$$

where $U_0\in S_0(U_1,U_0)$, $U_1\in\overrightarrow{R}_3(U_+,U)$, $\rho^*_9<\rho_1<\rho^*_{C_1}$. There exists a unique solution for (3.17) on the left side of S_0. See Figure 3.16 (right). The large-time behavior of the solution from the theory of isentropic gas dynamical system (2.5) is as follows

$$U_-\oplus\overleftarrow{R}_1(U_9,U_-)\oplus S_0(U_{9*},U_9)\oplus\overrightarrow{R}_3(U_+,U_{9*})\oplus U_+.$$

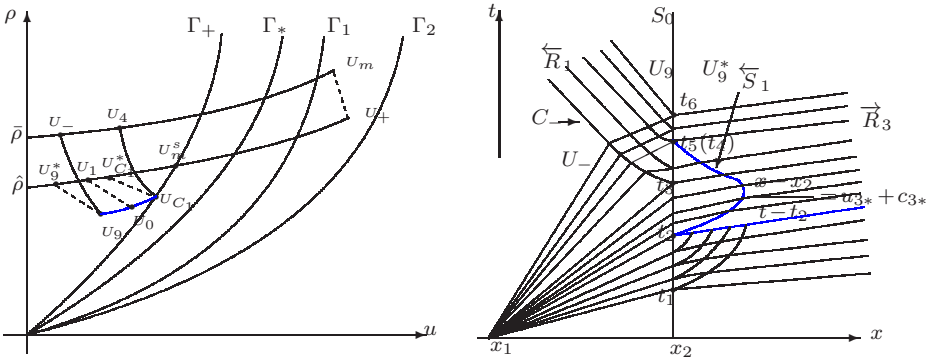

Fig. 3.16. The solutions for subcase 3.5.

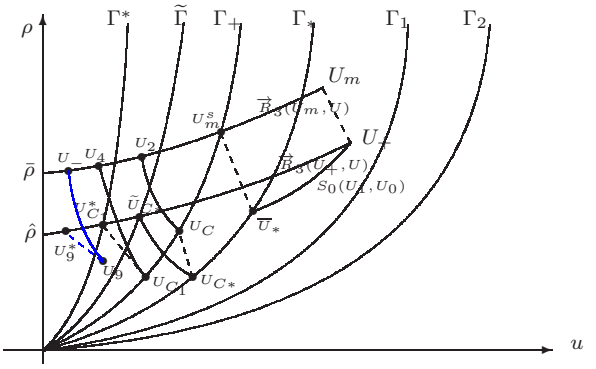

Fig. 3.17. Case 4. $(u_+,\rho_+)\in$ III.

Case 4. $U_+=(u_+,\rho_+)\in$ III. See Figure 3.17.

$S_0(U_1,U_0)$ is below $\overrightarrow{R}_3(U_+,U)$ in the supersonic area, touches Γ_* at $\overline{U}_*$. As case 3, we denote $\widetilde{U}_{C*}=\widetilde{\Gamma}\cap\overrightarrow{R}_3(U_+,U)$, $\widetilde{\Gamma}$ is denoted in (3.13). $\widetilde{U}_{C*}$ and $U_{C*}\in\Gamma_*$ are con-

nected by a zero-speed shock wave. U_{C*} and $U_C \in \Gamma_+$ are connected by a stationary wave $S_0(U_{C*},U_C)$. Denote $U_2 = \overleftarrow{R}_1(U_C,U) \cap \overrightarrow{R}_3(U_m,U)$. Then U_2 is a critical point. Denote $U^*_{C_1} = \overrightarrow{R}_3(U_+,U) \cap \Gamma^*$, which is obtained by U_{C_1} on Γ_+ with $S_0(U^*_{C_1},U_{C_1})$. $U_4 = \overrightarrow{R}_3(U_m,U) \cap \overleftarrow{R}_1(U_{C_1})$.

Subcase 4.1. U_- is between U_m and U^s_m on the curve $\overrightarrow{R}_3(U_m,U)$. We solve a free boundary value problem as (3.14) in the rectangular domain $\{(x,t)\big|x \geq x_2, t \geq t_1\}$. There exists a unique solution in the domain including a shock wave from the theory of the isentropic gas dynamical system. The large-time behavior of the solution is the same with subcase 3.2, see Figure 3.18.

Subcase 4.2. U_- is between U^s_m and U_2 (Figure 3.17). The interaction includes two parts. The first part from t_1 to t_2 is the same with subcase 4.1. In the second part from t_2 to t_3, we solve the boundary value problems as (3.11) and (3.14). A backward rarefaction wave reflects in this part and coincides with S_0, see Figure 3.18. The large time behavior of the solution is the same with subcase 3.3.

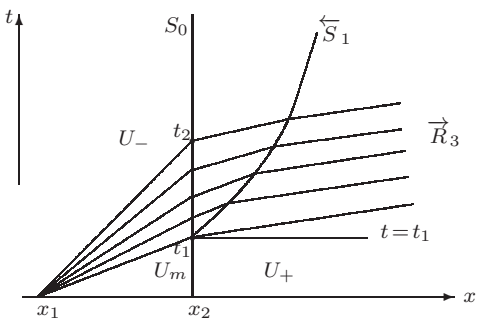

Fig. 3.18. The solutions for subcase 4.1.

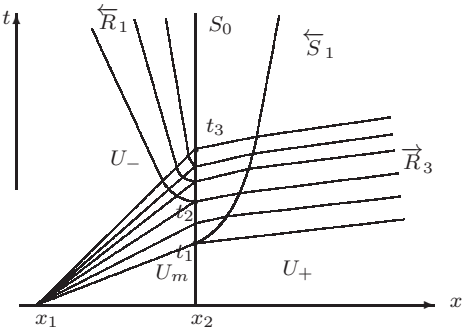

Fig. 3.19. The solutions for subcase 4.2.

Subcase 4.3. U_- is between U_2 and U_4 (Figure 3.17). The interaction includes three parts. The first two parts from time t_1 to t_3 are the same with subcase 4.2. When U_0 goes down along Γ_+ passing U_C, a shock wave $\overleftarrow{S}_1$ transmits during the interaction. The speed of $\overleftarrow{S}_1$ decreases in $\overrightarrow{R}_3$ from time t_1 to t_3. At the critical point $U_0 = U_C, U_1 = U_{C*}$, the speed equals to zero, and then become negative when U_0 is below U_C on the curve Γ_+, it keeps a constant negative speed after penetrating $\overrightarrow{R}_3$.

The third part is from t_3 to t_4, $\overleftarrow{S}_1$ penetrates $\overrightarrow{R}_3$ and touches S_0 during this period. Figure 3.20-1 shows the transition between subcase 4.2 and 4.3. On the one hand, U_- connects with U_A on Γ_+ through $\overleftarrow{R}_1(U_A,U_-)$, U_A jumps to U_{A*} by S_0, U_{A*} connects with U_8 on $\overrightarrow{R}_3(U_+,U))$ by a backward shock wave with negative speed: $\sigma_1(U_8,U_{A*}) < 0$. On the other hand, we solve a generalized Riemann problem as (3.15) at time $t = t_4$. The solution includes backward waves $\overleftarrow{R}_1$ and $\overleftarrow{S}_1$, which connect U_- and U_B. U_B jumps to U^*_B by stationary wave, and U^*_B connects with U_8 by a forward shock wave. Here U_B, U^*_B and U_8 are obtained by solving a similar problem as (3.15).

The shock wave $\overleftarrow{S}_1$ interacts with $\overleftarrow{R}_1$ and leaves $\overleftarrow{R}_1$ on the left of S_0 when $t \to +\infty$. On the right of S_0, $\overrightarrow{S}_3$ will interact with $\overrightarrow{R}_3$, a direct calculation shows that $\overrightarrow{S}_3$ does not cross $\overrightarrow{R}_3$ completely, see Figure 3.20-2.

When U_- is close to U_4, the speed of both $\overleftarrow{S}_1$ and $\overrightarrow{S}_3$ will decrease. At the critical case $U_- = U_4$, t_3 and t_4 coincide. We have $U_A = U_B = U_{C_1}$, $U^*_B = U_8 = U^*_{C_1}$ in this case, so there are no shock waves emitted when $t > t_5$. See Figure 3.21-1.

Subcase 4.4. U_- is between U_4 and $\bar{U}=(0,\bar{\rho})$ (Figure 3.17). The interaction includes three parts. The first two parts from t_1 to $t_3(t_4)$ are the same with subcase 4.3. The third part is from t_4 to t_5. At the time t_4, we solve a generalized Riemann solution as (3.16). There exists a unique solution including a backward rarefaction wave $\overleftarrow{R}_1$ connecting U_- and U_9, a stationary wave $S_0(U_{9*},U_9)$ and a forward rarefaction wave $\overrightarrow{R}_3$ connecting U_{9*} and U_+. See Figure 3.21-2. The large-time behavior of the solution from the theory of isentropic gas dynamical system (2.5) is

$$U_-\oplus\overleftarrow{R}_1(U_9,U_-)\oplus S_0(U_{9*},U_9)\oplus\overrightarrow{R}_3(U_+,U_{9*})\oplus U_+.$$

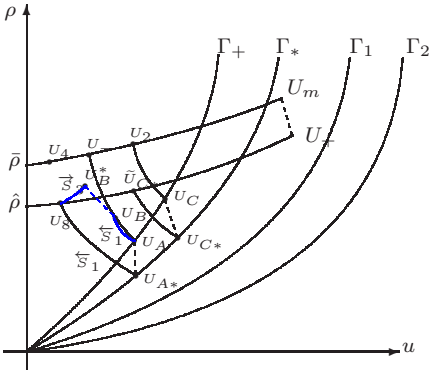

Fig. 3.20-1. The transition between the subcase 4.2-4.3.

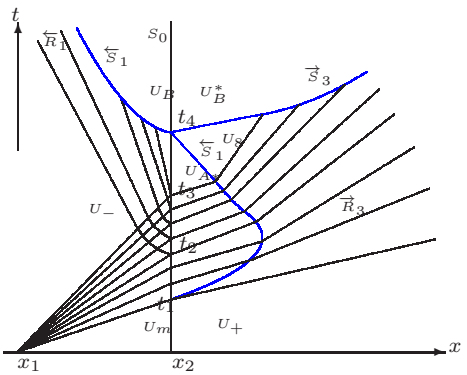

Fig. 3.20-2. The solutions for subcase 4.3.

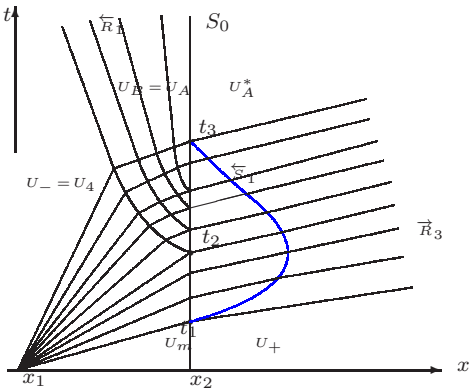

Fig. 3.21-1. The critical case $U_-=U_4$.

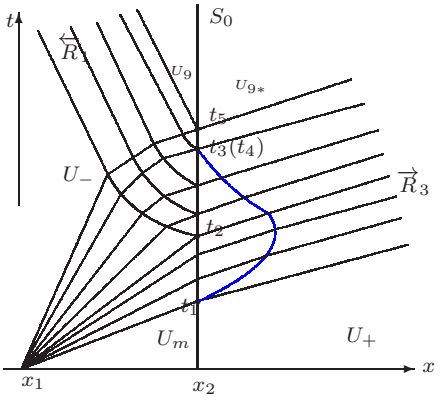

Fig. 3.21-2. The solutions for subcase 4.4.

Case 5. $U_+=(u_+,\rho_+)\in$ V. See Figure 3.22.

In the subsonic area, $S_0(U_1,U_0)$ is below $\overrightarrow{R}_3(U_+,U)$, touches ρ-axis at $\bar{U}=(0,\bar{\rho})$. The interaction process is from t_1 to t_2. $U_0^s\in\overleftarrow{S}_1(U,U_-)$, denote $U_2^*=S_0(U_1^s,U_0^s)\cap\overrightarrow{R}_3(U_+,U)$, which is obtained by $U_2\in\overleftarrow{S}_1(U,U_-)$. We solve the initial boundary value problem (2.5) with

$$(u,\rho)=\begin{cases}\left(\dfrac{2}{\gamma+1}\left(\xi-c_-+\dfrac{\gamma-1}{2}u_-\right),\left(\dfrac{(\xi-u)^2}{\kappa\gamma}\right)^{\frac{1}{\gamma-1}}\right), & t=t_1,x<x_2,\\ U_0=(u_0,\rho_0), & t_1<t<t_2,x=x_2,\\ U_2, & t>t_2,x=x_2,\end{cases}\tag{3.18}$$

where $U_0 \in S_0(U_1,U_0)$ is obtained by $U_1 \in \overrightarrow{R}_3(U_+,U)$ (U_1 is the right-hand state). The solution of (3.18) contains a reflecting shock wave. See Figure 3.23. The large-time behavior of the solution from the isentropic gas dynamical system theory is

$$U_- \oplus \overleftarrow{S}_1(U_2,U_-) \oplus S_0(U_2^*,U_2) \oplus \overrightarrow{R}_3(U_+,U_2^*) \oplus U_+.$$

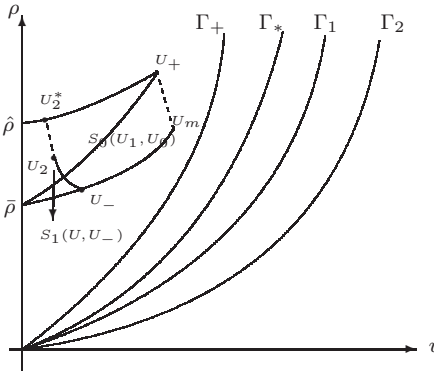

Fig. 3.22. Case 5. $(u_+,\rho_+) \in \mathrm{V}$.

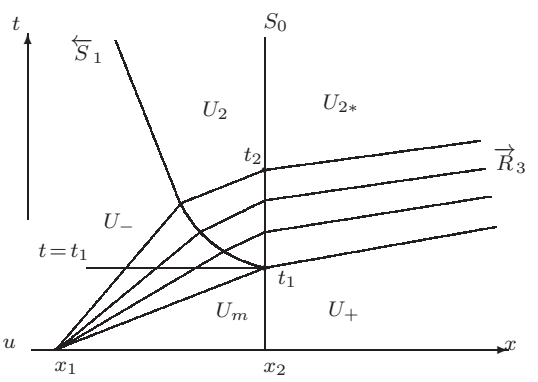

Fig. 3.23. The solution for Case 5.

3.2. The interaction of shock wave with stationary wave. In this section, we also consider the initial value problem of (1.1) with (3.1). $U_m \in \overrightarrow{S}_3(U,U_-)$, $U_+ \in S_0(U,U_m)$, we have

$$\overrightarrow{S}_3(U_m,U_-): \begin{cases} u_- = u_m + \left(\kappa\left(\dfrac{1}{\rho_m}-\dfrac{1}{\rho_-}\right)(\rho_-^\gamma - \rho_m^\gamma)\right)^{1/2}, \quad \rho_- > \rho_m, \\ \sigma_3(U_m,U_-) = u_- + \left(\dfrac{\rho_m}{\rho_-}\dfrac{p_m-p_-}{\rho_m-\rho_-}\right)^{1/2} > 0, \end{cases} \tag{3.19}$$

$$S_0(U_+,U_m): \begin{cases} a_0\rho_m u_m = a_1\rho_+ u_+, \\ u_m^2 + \dfrac{2\kappa\gamma\rho_m^{\gamma-1}}{\gamma-1} = u_+^2 + \dfrac{2\kappa\gamma\rho_+^{\gamma-1}}{\gamma-1}, \\ \sigma_0 = 0. \end{cases} \tag{3.20}$$

The state $U=(u,\rho) \in \overrightarrow{S}_3(U_+,U)$ (U_+ is the right-hand state) is given by:

$$u(\rho) = u_+ + \left(\kappa\left(\frac{1}{\rho_+}-\frac{1}{\rho}\right)(\rho^\gamma - \rho_+^\gamma)\right)^{\frac{1}{2}}, \quad \rho > \rho_+.$$

From (3.19) and (3.20), we have $\sigma_3(U_m,U_-) > \sigma_0 = 0$, which means $\overrightarrow{S}_3$ will overtake S_0.

Liu [15,16] has concluded that flows along an expanding duct are stable. Moreover, he has proved that shock waves tend to decelerate along an expanding duct, which is equivalent to $\sigma_3(U_m,U_-) > \sigma_3(U_+,U)$ here. We discuss the interactions case by case.

Case 1. U_m,U_+ are on the right of Γ_+. So we have $u_m > c_m, u_+ > c_+$, and $u_m < u_+$ when the cross section increases. When $\overrightarrow{S}_3(U_m,U_-)$ overtakes $S_0(U_+,U_m)$, we solve a new Riemann problem of (1.1) with

$$(u,\rho,a)\Big|_{t=t_1} = \begin{cases} U_- = (u_-,\rho_-,a_0), & x < x_2, \\ U_+ = (u_+,\rho_+,a_1), & x > x_2. \end{cases} \tag{3.21}$$

This case indicates that U_- will jump to U_{-*} by S_0 first. According to relative position of U_{-*} and $\overrightarrow{S}_3(U_+,U)$, we discuss as follows.

Case 1.1. U_{-*} is on the left of $\overrightarrow{S}_3(U_+,U)$ (Figure 3.24). Then U_- jumps to U_{-*} by S_0 first, then U_{-*} connects with U_1 by $\overleftarrow{R}_1(U,U_{-*})$, finally U_1 jumps to U_+ by $\overrightarrow{S}_3(U_+,U_1)$.

$$\overrightarrow{S}_3(U_m,U_-)\oplus S_0(U_+,U_m)\to S_0(U_{-*},U_-)\oplus \overleftarrow{R}_1(U_1,U_{-*})\oplus \overrightarrow{S}_3(U_+,U_1).$$

Which means that the forward shock wave will transmit a backward rarefaction wave when it penetrates the stationary wave.

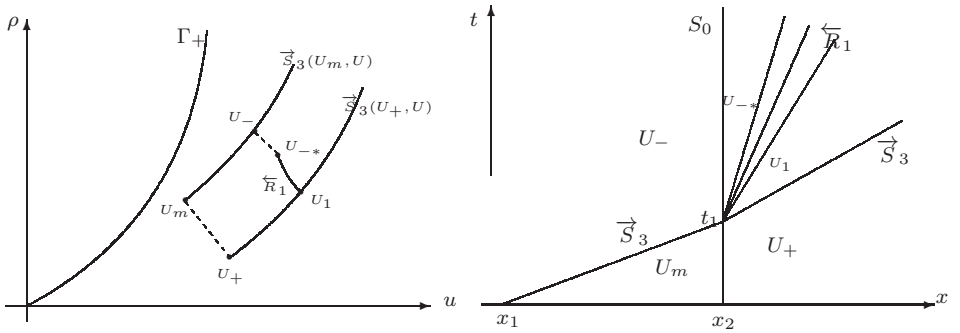

Fig. 3.24. U_{-*} is on the left of $S_3(U_+,U)$.

Case 1.2. U_{-*} is on the right of $\overrightarrow{S}_3(U_+,U)$ (Figure 3.25). Then U_- jumps to U_{-*} by S_0 first, U_{-*} connects with U_2 by $\overleftarrow{S}_1(U,U_{-*})$, finally U_2 jumps to U_+ by $\overrightarrow{S}_3(U_+,U_2)$.

The solution for (3.21) in this case is

$$\overrightarrow{S}_3(U_m,U_-)\oplus S_0(U_+,U_m)\to S_0(U_{-*},U_-)\oplus \overleftarrow{S}_1(U_2,U_{-*})\oplus \overrightarrow{S}_3(U_+,U_2).$$

Which means that the forward shock wave will transmit a backward shock wave when it penetrates the stationary wave.

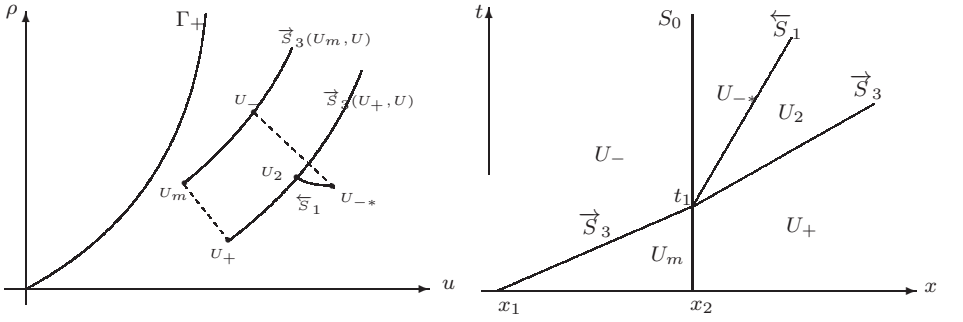

Fig. 3.25. U_{-*} is on the right of $S_3(U_+,U)$.

Case 2. $u_m<c_m, u_+<c_+$ and $u_-<c_-$ (Figure 3.26). Here we choose the subsonic solution when using the stationary wave. We discuss the results as follows.

Case 2.1. U_-^* is below $\overrightarrow{S}_3(U_+,U)$. U_- connects with U_3 by $\overleftarrow{S}_1(U_3,U_-)$, U_3 jumps to

U_3^* by $S_0(U_3^*,U_3)$, finally U_3^* jumps to U_+ by $\overrightarrow{S}_3(U_+,U_3^*)$. See Figure 3.26. The states U_3 and U_3^* are determined by

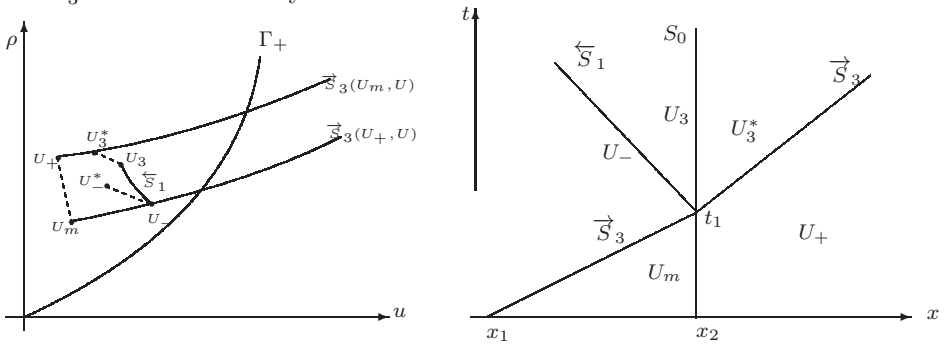

Fig. 3.26. U_-^* is below $\overrightarrow{S}_3(U_+,U)$.

$$\begin{cases} \dfrac{\mathrm{d}x}{\mathrm{d}t}=u_- -\left(\dfrac{\rho_3(p(\rho_3)-p(\rho_-))}{\rho_-(\rho_3-\rho_-)}\right)^{\frac{1}{2}}, \\ u_3=u_- -\left(\kappa\left(\dfrac{1}{\rho_-}-\dfrac{1}{\rho_3}\right)\left(\rho_3^\gamma-\rho_-^\gamma\right)\right)^{\frac{1}{2}}, \end{cases} \quad (\text{the R}-\text{H condition of } \overleftarrow{S}_1(\mathrm{U}_3,\mathrm{U}_-))$$

$$\begin{cases} a_0\rho_3u_3=a_1\rho_3^*u_3^*, \\ \dfrac{u_3^2}{2}+\dfrac{c_3^2}{\gamma-1}=\dfrac{u_3^{*2}}{2}+\dfrac{c_3^{*2}}{\gamma-1}, \end{cases} \quad (U_3,U_3^*\in S_0(U_3^*,U_3))$$

$$\begin{cases} u_3^*=u_+ +\left(\kappa\left(\dfrac{1}{\rho_3^*}-\dfrac{1}{\rho_+}\right)\left(\rho_+^\gamma-\rho_3^{*\gamma}\right)\right)^{\frac{1}{2}}, \\ \rho_3^*>\rho_+, \end{cases} \quad (\text{the R}-\text{H condition of } \overrightarrow{S}_3(U_+,U_3^*)).$$

The solution of (3.21) in this case is

$$\overrightarrow{S}_3(U_m,U_-)\oplus S_0(U_+,U_m)\to\overleftarrow{S}_1(U_3,U_-)\oplus S_0(U_3^*,U_3)\oplus\overrightarrow{S}_3(U_+,U_3^*),$$

which means that the forward shock wave will reflect a backward shock wave when it penetrates the stationary wave.

Case 2.2. U_-^* is above $\overrightarrow{S}_3(U_+,U)$. We denote $U_c=\overleftarrow{R}_1(U,U_-)\cap\Gamma_+$, see Figure 3.27.

If U_c^* is below $\overrightarrow{S}_3(U_+,U)$, then U_- connects with U_4 by $\overleftarrow{R}_1(U_4,U_-)$, U_4 jumps to U_4^* by $S_0(U_4^*,U_4)$, finally U_4^* jumps to U_+ by $\overrightarrow{S}_3(U_+,U_4^*)$. The states U_4 and U_4^* are determined by

$$\begin{cases} u_4+\dfrac{2c_4}{\gamma-1}=u_-+\dfrac{2c_-}{\gamma-1}, & (\text{the Riemann invariant of } \overleftarrow{R}_1(U_4,U_-)). \\ \begin{cases} a_0\rho_4u_4=a_1\rho_4^*u_4^*, \\ \dfrac{u_4^2}{2}+\dfrac{c_4^2}{\gamma-1}=\dfrac{u_4^{*2}}{2}+\dfrac{c_4^{*2}}{\gamma-1}, \end{cases} & (U_4,U_4^* \text{ are connected by } S_0(U_4^*,U_4)) \\ \begin{cases} u_4^*=u_+ +\left(\kappa\left(\dfrac{1}{\rho_4^*}-\dfrac{1}{\rho_+}\right)\left(\rho_+^\gamma-\rho_4^{*\gamma}\right)\right)^{\frac{1}{2}}, \\ \rho_4^*>\rho_+, \end{cases} & (\text{the R}-\text{H condition of } \overrightarrow{S}_3(U_+,U_3^*)). \end{cases} \tag{3.22}$$

The solution of (3.21) is

$$\overrightarrow{S}_3(U_m,U_-)\oplus S_0(U_+,U_m)\to\overleftarrow{R}_1(U_4,U_-)\oplus S_0(U_4^*,U_4)\oplus\overrightarrow{S}_3(U_+,U_4^*),$$

which means that the forward shock wave will reflect a backward rarefaction wave when it penetrates the stationary wave.

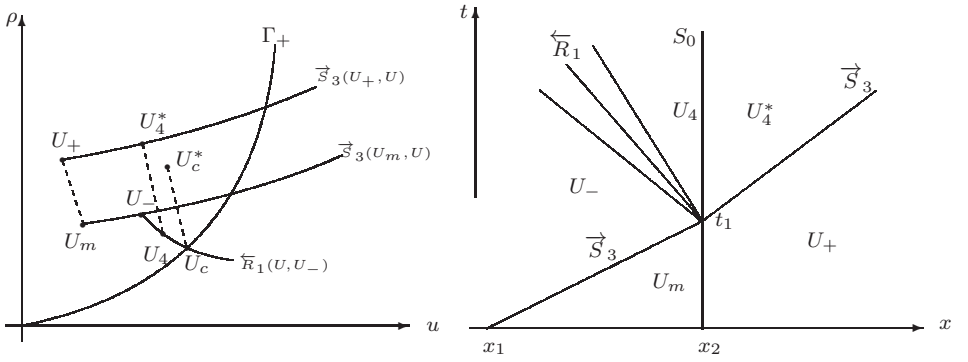

Fig. 3.27. U_-^* is above $\overrightarrow{S}_3(U_+,U)$, U_c^* is below $\overrightarrow{S}_3(U_+,U)$.

If U_c^* is above $\overrightarrow{S}_3(U_+,U)$ (Figure 3.28), U_- connects with U_c by $\overleftarrow{R}_1(U_c,U_-)$, U_c jumps to U_{c*} by $S_0(U_{c*},U_c)$, and U_{c*} jumps to U_5 by $\overrightarrow{S}_1(U_5,U_{c*})$ with $\sigma_1(U_5,U_{c*})>0$, finally U_5 connects with U_+ by $\overrightarrow{S}_3(U_+,U_5)$. U_{c*} and U_5 can be determined as (3.22).

$$\overrightarrow{S}_3(U_m,U_-)\oplus S_0(U_+,U_m)\to\overleftarrow{R}_1(U_c,U_-)\oplus S_0(U_{c*},U_c)\oplus\overrightarrow{S}_1(U_5,U_{c*})\oplus\overrightarrow{S}_3(U_+,U_5).$$

This case means that the forward shock wave will reflect a backward rarefaction wave, it will coincide with the stationary wave and transmit a backward shock wave.

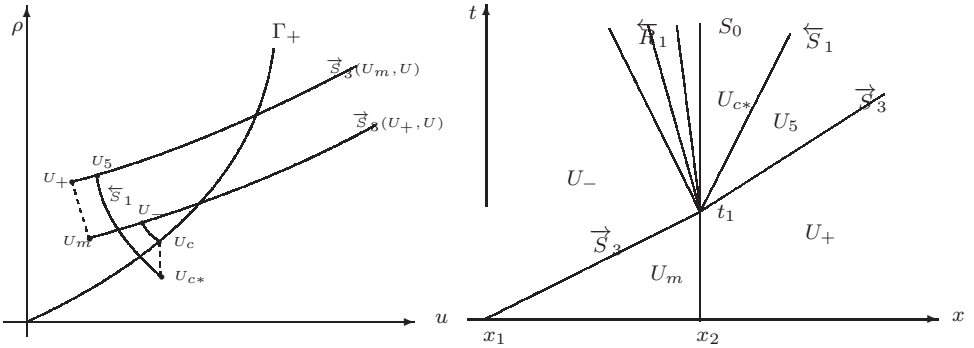

Fig. 3.28. U_-^* is above $\overrightarrow{S}_3(U_+,U)$, U_c^* is above $\overrightarrow{S}_3(U_+,U)$

Case 3. $u_m<c_m, u_+<c_+$ and $u_->c_-$. See Figure 3.29-30. We discuss the results as follows.

Case 3.1. Denote $\widetilde{U}_-\in\overleftarrow{S}_1(U,U_-)$ which satisfies $\sigma_1(\widetilde{U}_-,U_-)=0$, $\widetilde{U}_-$ jumps to $\widetilde{U}_-^*$ by $S_0(\widetilde{U}_-^*,\widetilde{U}_-)$. If $\widetilde{U}_-^*$ is below $\overrightarrow{S}_3(U_+,U)$, then U_- will first jump to U_6 above $\widetilde{U}_-$ by $\overleftarrow{S}_1(U_6,U_-)$ with $\sigma_1(U_6,U_-)<0$, U_6 jumps to U_6^* by $S_0(U_6^*,U_6)$, finally U_6^* connects with U_+ by $\overrightarrow{S}_3(U_+,U_6^*)$. See Figure 3.29.

$$\overrightarrow{S}_3(U_m,U_-)\oplus S_0(U_+,U_m)\to\overleftarrow{S}_1(U_6,U_-)\oplus S_0(U_6^*,U_6)\oplus\overrightarrow{S}_3(U_+,U_6^*).$$

The interaction result is the same as in Figure 3.26.

Case 3.2. U_- jumps to U_{-*} by $S_0(U_{-*},U_-)$. Denote $\widetilde{U}_{-*}\in \overleftarrow{S}_1(U,U_{-*})$ which satisfies $\sigma_1(\widetilde{U}_{-*},U_{-*})=0$. If $\widetilde{U}_{-*}$ is above $\overrightarrow{S}_3(U_+,U)$, then U_{-*} jumps to U_7 by $\overleftarrow{S}_1(U_7,U_{-*})$ with $\sigma_1(U_7,U_{-*})>0$, U_7 connects with U_+ by $\overrightarrow{S}_3(U_+,U_7)$.

$$\overrightarrow{S}_3(U_m,U_-)\oplus S_0(U_+,U_m)\to S_0(U_{-*},U_-)\oplus \overleftarrow{S}_1(U_7,U_{-*})\oplus \overrightarrow{S}_3(U_+,U_7).$$

The interaction result is the same as in Figure 3.25.

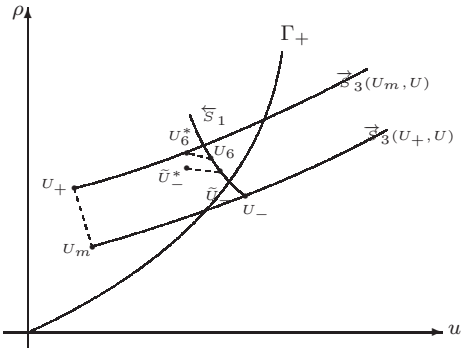

Fig. 3.29. $\widetilde{U}_-^*$ is below $\overrightarrow{S}_3(U_+,U)$.

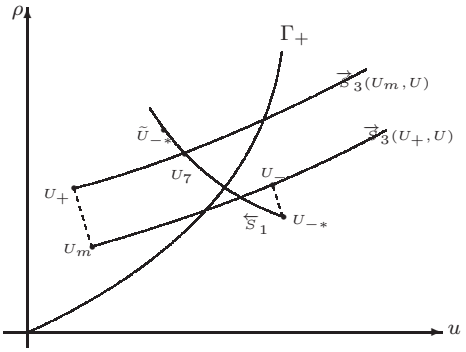

Fig. 3.30. $\widetilde{U}_{-*}$ is above $\overrightarrow{S}_3(U_+,U)$.

In summary, we have obtained the results of rarefaction wave as well as shock wave interactions with the stationary wave in a variable cross-section duct. When a forward rarefaction wave interacts with a stationary wave, it will transmit a forward rarefaction wave. During the process, a backward wave will transmit or reflect as well. When the transmitted wave is a backward compressible shock wave, we further discuss the shock intensity by solving free boundary problems. When a forward shock wave interacts with a stationary wave, it will penetrate the stationary wave, and either transmit or reflect a backward rarefaction wave or shock wave.

Acknowledgment. The authors are thankful to the referees' helpful comments.

REFERENCES

[1] N. Andrianov and G. Warnecke, *On the solution to the Riemann problem for the compressible duct flow*, SIAM J. Appl. Math., 64:878–901, 2004.
[2] M.R. Baer and J.W. Nunziato, *A two-phase mixture theory for the deflagration-to-detonation transition (DDT) in reactive granular materials*, Int. J. Multiphase Flows, 12:861–889, 1986.
[3] T. Chang and L. Hsiao, *The Riemann Problem and Interaction of Waves in Gas Dynamics*, Pitman Monographs, Longman Scientific and technica, 41:95–161, 1989.
[4] G. Dal Maso, P.G. LeFloch, and F. Murat, *Definition and weak stability of nonconservative products*, J. Math. Pures Appl., 74(9):483–548, 1995.
[5] P. Goatin and P.G. LeFloch, *The Riemann problem for a class of resonant hyperbolic systems of balance laws*, Ann. Inst. H. Poincare Anal. Non Lineaire, 21:881–902, 2004.
[6] E. Isaacson and B. Temple, *Convergence of the* 2×2 *Godunov method for a general resonant nonlinear balance law*, SIAM J. Appl. Math., 55:625–640, 1995.
[7] E. Isaacson and B. Temple, *Nonlinear resonance in systems of conservation laws*, SIAM J. Appl. Math., 52:1260–1278, 1992.
[8] D. Kröner and M.D. Thanh, *Numerical solutions to compressible flows in a nozzle with variable cross–section*, SIAM J. Numer. Anal., 43:796–824, 2005.
[9] D. Kröner, P.G. LeFloch, and M.D. Thanh, *The minimum entropy principle for fluid flows in a nozzle with discontinuous cross-section*, M2AN Math. Model Numer. Anal., 42:425–442, 2008.
[10] P. Lax, *Shock waves and entropy*, in "Contributions to Functional Analysis", E.A. Zarantonello (ed.), Academic Press, New York, 603–634, 1971.

[11] P.G. LeFloch, *Shock waves for nonlinear hyperbolic systems in nonconservative form*, Preprints Series, Institute for Mathematics and its Application, Minneapolis, 593, 1989.
[12] P.G. LeFloch and M.D. Thanh, *The Riemann problem for fluid flows in a nozzle with discontinuous cross-section*, Commun. Math. Sci., 1:763–797, 2003.
[13] P.G. LeFloch and A.E. Tzavaras, *Representation of weak limits and definition of nonconservative products*, SIAM J. Math. Anal., 30:1309–1342, 1999.
[14] T.T. Li and W.C. Yu, *Boundary value problems of quasilinear hyperbolic system*, Duke University Mathematics Series 5, Duke University, USA, 1985.
[15] T.P. Liu, *Transonic gas flow in a duct of varying area*, Arch. Rat. Mech. Anal., 80:1–18, 1982.
[16] T.P. Liu, *Nonlinear stability and instability of transonic flows through a nozzle*, Comm. Math. Phys., 83:243–260, 1982.
[17] D. Marchesin and P.J. Paes–Leme, *A Riemann problem in gas dynamics with bifurcation. Hyperbolic partial differential equations, III*, Comput. Math. Appl. Part A, 12:433–455, 1986.
[18] R. Saurel and R. Abgrall, *A multiphase Godunov method for compressible multifluid and multiphase flows*, J. Comput. Phys., 150:425–467, 1999.
[19] R. Saurel and R. Abgrall, *A simple method for compressible multifluid flows*, SIAM J. Sci. Comput., 21:1115–1145, 1999.
[20] M.D. Thanh, *The Riemann problem for a nonisentropic fluid in a nozzle with discontinuous cross-sectional area*, SIAM J. Appl. Math., 69:1501–1519, 2009.
[21] R.H. Wang and Z.Q. Wu, *Existence and uniqueness of solutions for some mixed initial boundary value problmes of quasilinear hyperbolic systems in two independent variables*, (in Chinese), Acta Scientiarum Naturalium of Jilin University, 2:459–502, 1963.